ACOUSTIC DETECTION OF AIRCRAFT FROM AN AIRBORNE PLATFORM

JESSE ROSS-JONES

Acoustic Detection of Aircraft from an Airborne Platform

by

©Jesse Ross-Jones

B.Eng., University of Waterloo, Canada (2010)

A thesis submitted to the
School of Graduate Studies
in partial fulfillment of the
requirements for the degree of
Master of Engineering

Faculty of Engineering and Applied Science
Memorial University of Newfoundland

May 2012

St. John's Newfoundland

Acoustic Detection of Aircraft from an Airborne Platform

by

Jesse Ross-Jones

Abstract

The question to be answered, was: Is it possible to develop an acoustic UAS system able to operate in adverse environmental conditions such as fog, to detect oncoming aircraft and provide the ability for successful avoidance? As a result of the lack of sense and avoid capability, Unmanned Aerial Systems are restricted to fly within line of sight of the operator limiting its utility. Various sensors are researched for sense and avoid, including Electro-Optical (EO) and Infrared (IR) cameras, as well as acoustic, radar and electromagnetic sensors. Acoustic sensors were the focus of this thesis.

This question was addressed. The three main experiments conducted were able to show that a sound source could be localized using an arrangement of 4 microphones. Furthermore, a ground test followed by an airborne test was conducted which showed a moving craft could detect the sound source. The detection distance was approximately 42 meters. Using the detection distances from the ground and airborne experiments, and the sound levels for manned aircraft, an estimate was made for the detection distance of a manned aircraft: a Cessna is approximated to be at a distance of 4761 meters, a Shadow UAV would be approximately 500 meters away.

Acknowledgements

This thesis would not have been possible without the support of Siu O'Young. Without his enthusiasm, his inspiration, new ideas and supervision this thesis would not be what it is today. I owe my deepest gratitude to Armin Stobel whose wise advice and support kept me going. I owe profound thanks to Charlotte Capitain for pushing me forward and without whom those days in the library would have been simply unbearable. It is a pleasure to thank those who made this thesis possible, Scott Fang, Gayan Gamage, Yu Liu, Daniel Zanker, Stephen Crewe, Kevin Murrant, Dilhan Balage, Robert MacIsaac, Kaaren May, Michael Bakula, Michael Vohla, Raju Hossain, Muthu Gandi, Nancy Leawood, Jordan Peckham, my stimulating and fun colleagues whose support, camaraderie and entertainment was invaluable. I am grateful to David Snook, Robert Murphy and Brian Pretty for their technical support. I would like to thank Len Zedel and Rene Lange for their ideas and support, as well as Ralf Bachmayer for talking to me about his work. I would like to show my gratitude to Scott Foster who helped me getting started with the audio analysis and recording. I would also like to thank Joanna Fyans, Lakmal Siriwardana and Zhenlong (Lancy) Cheng for the exhausting badminton matches. Lastly, it is an honour for me to thank my sisters, Jennifer and Joy as well as my father and mother, James and Sharon Ross-Jones, for their love and never ending support. Thank you, I love you.

Contents

Abstract i

Acknowledgements ii

Contents iii

List of Figures vi

List of Tables ix

1 Introduction 1

1.1 UAS 1

1.2 Aircraft Sensors 2

1.2.1 EO/IR Sensors 2

1.2.2 Radar 4

1.2.3 Acoustic Localization 4

1.3 Problem Statement 5

1.4 Outline 5

1.5 Challenges 6

2 Background and Literature Review 7

2.1 Acoustic Concepts 7

2.1.1 Sound Propagation 7

2.1.2 Aircraft Sound . . . 8
2.1.3 Acoustic Data Analysis . . . 10
2.1.4 Fourier Transform . . . 10
2.1.5 Sound Source Localization . . . 11
2.1.6 Target Detection . . . 15
2.1.7 Improvements in Microphone Technology . . . 16
2.2 Fluid Dynamics . . . 20
2.2.1 Laminar and turbulent flow . . . 20
2.2.2 NACA airfoil design . . . 20

3 Design of the Airborne Payload **22**
3.1 Tetrahedron Method . . . 22
3.2 Noise Level Simulation and Signal to Noise Ratio . . . 27
3.3 Design Of Experiments . . . 28
3.4 Design of Capsule . . . 29
3.4.1 Aerodynamics of Capsule . . . 29
3.4.2 Manufacture of capsule . . . 31
3.5 Microphone Capsule Experiment . . . 31
3.5.1 The Experiment . . . 31

4 Data and Analysis **36**
4.1 Localization Experiment . . . 36
4.1.1 Tetrahedron Data . . . 36
4.1.2 Tetrahedron Analysis . . . 38
4.2 Ground Experiment . . . 42
4.2.1 Frequency Response . . . 42
4.2.2 Ground Experiment Data . . . 44
4.2.3 Ground Experiment Analysis . . . 47
4.3 Airborn Experiment . . . 53

4.3.1 Capsule Air Data 53

5 Results **60**

5.1 Tetrahedron Results 60

5.2 Ground and Air Tests 60

6 Conclusions and Future Work **65**

6.1 Conclusions 65

6.2 Future work 66

Bibliography **67**

A Diagrams **71**

A.1 Microphone Capsule Design and Manufacture 71

A.2 Spectrograms of GoPro and Capsule audio recordings 73

A.3 Design Expert Diagrams 76

B Equipment Used **80**

B.1 Tetrahedron Experiment 80

B.2 Ground Experiment 80

B.3 Airborne Experiment 81

List of Figures

2-1 Temperature Effect on Sound Wave Propagation 8
2-2 Attenuation of Sound due to Temperature and Humidity 9
2-3 Incident Wave Geometry 12
2-4 Acoustic Velocity Sensor 18
2-5 Acoustic Sense and Avoid Systems 19

3-1 Normalized Phase Correlation 24
3-2 Localization Cone 26
3-3 Minimum Signal to Noise Ratio 27
3-4 NACA 16-012 Boundary Layer Analysis 30
3-5 NACA 16-012 Angle of Attack Analysis 32
3-6 Airfoil 3D Model 33
3-8 Microphone Placed inside Fiberglass Enclosure 34

4-1 Detected Frequency Peaks 37
4-2 Spectrogram of Recorded Flyby 38
4-3 Model of Acoustic Array 39
4-4 Normalized Phase Correlation 41
4-5 Angle of Arrival 41
4-6 Frequency Spectrogram of Microphone Capsule Designs 43
4-7 Frequency Response Comparison of Microphone Capsule Designs . . . 44
4-8 Frequency Response using the GoPro Camera 45

4-9 Vehicle Setup for Ground Based Test 45
4-10 Microphone Setup for Ground Based Test 46
4-11 Microphone Setup for Ground Based Test 46
4-12 Drive-by for Ground Based Test 47
4-13 50 kilometres per hour and 10 meter separation 48
4-14 ANOVA results 50
4-15 ANOVA results 50
4-16 Car Horn Sound Levels 52
4-17 Acoustic Air Experiment 55
4-18 Airborne Experiment Flight Track 56
4-19 Airborne Experiment Spectrogram 56
4-20 Acoustic Weighting Curves 58
4-21 Car Horn Sound Levels 59

5-1 Delay from X Axis Microphone 61
5-2 Delay from Y Axis Microphone 61
5-3 Delay from Z Axis Microphone 62
5-4 3D Sound Source Direction @ Time = t 62

A.1 3D Printed NACA Airfoil 71
A.2 Completed Mold (Top and Bottom) 72
A.3 Microphone Capsule 72
A.4 50 kilometres per hour and 10 meter separation 73
A.5 20 kilometres per hour and 10 meter separation 74
A.6 50 kilometres per hour and 20 meter separation 74
A.7 40 kilometres per hour and 20 meter separation 75
A.8 20 kilometres per hour and 20 meter separation 75
A.9 Normal Plot of Residuals 76
A.10 Residuals vs Predicted 77

A.11 Residuals vs Run 78
A.12 Box Cox Plot 79

List of Tables

2.1 Estimated Sound Levels for Various Aerial Craft 9

3.1 Variable descriptions and units 26

4.1 GoPro Ground Test Results 48
4.2 Microphone Capsule Ground Test Results 49
4.3 Cessna 182 Sound Levels 51
4.4 GoPro Ground Test Analysis 53
4.5 Microphone Capsule Ground Test Analysis 53
4.6 GPS Recorded Data 57

5.1 Microphone Capsule Ground Results 63
5.2 Microphone Capsule Airborne Results 63

Chapter 1

Introduction

1.1 UAS

Unmanned Aerial Systems (UAS) are currently restricted to fly within line of sight of the manned operator, and consequently, its capabilities are not fully utilized. Researching collision avoidance for beyond visual- range mission is divided into two areas, "sense" and "avoid". "Sense" involves the actual detection of intruders while "avoid" involves the taking of a proper course of action. The focus of my research is in the "sense" area. The Raven II project has authority from Transport Canada to conduct near mid-air collision (NMAC) encounters, allowing collection of data not available in other countries. Raven II Project is a Newfoundland based research project under the direction of Dr. Siu O'Young. The focus of the research is on Sense and Avoid for Unmanned Aerial Vehicles. In addition, Raven II has the capability of building custom aircraft to fit non standard payloads. Current work include: research in EO/IR and acoustic detection and Millimeter-wave radar is being tested as a possible payload for larger unmanned aircraft.

The detection of intruding aircraft and their classification is part of collision avoidance. To accomplish this task there are a variety of sensors that can be used. These sensors include Electro-Optical (EO) and Infrared (IR) cameras, as well as acoustic,

radar and electromagnetic sensors [1]. The use of one sensor exclusively for sensing has disadvantages. For example, EO cameras are difficult to use for sensing aircraft in the presence of fog and during nighttime, whereas IR sensors are capable of working at night and acoustic sensors in foggy conditions. However IR and acoustic sensors both have limited resolution [2]. More information is provided in Section 1.2.1.

Various general challenges exist in this research. One such challenge to the research is the necessary fast detection time required for successful avoidance, since potential incoming aircraft can travel at high relative velocities; the amount of time available to detect the intruding aircraft is very limited. Furthermore, an obstacle the Raven II project needs to overcome is performance working in a fog environment; the frequency of fog conditions in Newfoundland provide the group ample opportunity to develop working "sense" systems for fog challenged conditions.

1.2 Aircraft Sensors

1.2.1 EO/IR Sensors

One active area of research for "sense and avoid" is in the area of EO and IR cameras. Through the use of cameras placed strategically on the aircraft, researchers are working to improve detection algorithms and capabilities in order to sense an approaching aircraft visually. This approach has many advantages as well as various disadvantages and difficulties [3].

There are various advantages to using EO and IR cameras for "sense and avoid". Firstly, there are a great many resources dedicated to computer vision, including research into target detection. As well, there are a significant number of researchers continuously working to improve the algorithms and methods in this area [2]. Furthermore, there are a number of tools available to researchers in computer vision, including the Matlab Computer Vision toolbox as well as OpenCV, a cross platform development tool including a large number of implemented functions. When com-

pared with other detection systems such as radar, a camera implementation for "sense and avoid" is relatively light and low power. As well, cameras can be customized to provide different fields of view, sensor sizes, focal lengths, zoom capabilities and can be scaled to include more cameras and different perspectives. Lastly, one of the significant advantages of using IR cameras for detection is that aircraft show up quite well in the infra red image [3].

Computer vision research is not without its challenges, however. As the required detection distance increases so must the resolution of the camera. Furthermore, the camera used must have a large enough field of view in order to be able to scan enough of the visible sky to detect an approaching aircraft. As both of these factors, resolution and field of view, increase, so must the processing time/processing power increase (which can be mitigated through the use of GPU (Graphics processing unit) acceleration). Indeed, any algorithm used for target detection is prone to errors. As the camera must scan the sky for moving objects, it is possible, for example, to mistake an object on the ground for a moving aircraft. Thus, it is necessary to choose the right tools, which is made difficult as each algorithm can be susceptible to different environmental conditions, such as clouds in the sky, flying over land or water, fog and amount of light exposure. Consequently, the algorithms must be calibrated for the different flying conditions and likely, before each flight, the parameters of the algorithm changed to suit the current flying conditions. Furthermore, camera implementations are limited to 2D detection only, as the baseline between cameras on a single craft is too small to be able to ascertain range information on any air targets detected [2].

Some further difficulties exist for the use of IR cameras. For IR cameras with higher resolutions and frame rates, ITAR (International Traffic in Arms Regulations) restrictions exist which restrict the import and export of the equipment. This means that civilian and commercial applications are not likely without proper security clearances and paperwork; these applications are thus limited to the lower resolution and

frame rate IR cameras [3].

1.2.2 Radar

Another area of research for "sense and avoid" is Radar. Radar provides a significant advantage as it can be used in all weather conditions and during all times of the day. Furthermore, the potential detection range is dependant on the platform used. Larger aircraft are able to carry larger, more powerful radar systems. A larger platform will be able to carry a larger antenna capable of extending the detection range. Moreover, radar is able to detect and identify different types of targets, both in the air and on the ground. Processing the radar data is also quite fast as a target's direction is based on the position of the radar antenna and angular resolution of the antenna [4].

The significant drawback to radar systems however is in the size and power requirement of the system. Making radar systems for small unmanned systems is quite a challenge, since as the size and power decrease so does the detection range of the system [4].

1.2.3 Acoustic Localization

A third area of research for "sense and avoid" is in acoustic detection. There are various advantages to using microphones for detection of aircraft as well as significant drawbacks.

Similar to radar, acoustic sensors can be used in foggy conditions as well as during all times of the day. Another significant advantage that acoustic sensors have over radar and camera systems is in the field of view. An acoustic system can be used to detect an approaching aircraft regardless of its direction of approach. Moreover, the acoustic sensors do not need to be moved and can remain stationary, reducing the size of the system since no moving mechanical parts are required. Another advantage of acoustic detecting is processing speed. Acoustic data can be processed live with relative ease and can even be transmitted back to the ground if necessary. An acoustic

sensor is also a passive sensor, as opposed to radar which is an active sensor. This allows for lower power requirements, which is also ideal for situations where stealth is required.

Acoustic detection also has significant drawbacks. The foremost challenge is the amount of noise that is recorded by the microphones. Noise comes from not only the aircraft engine or motor, but also from vibrations of the platform, as well as significant noise from the wind. While some noises, such as the aircraft engine noise, can be managed by filtering out the relevant frequencies, the wind noise and vibrations exist across many frequencies and must be managed mechanically.

1.3 Problem Statement

The fundamental question is: is it possible to develop an acoustics based UAS detection system able to operate in adverse climatic/environmental conditions such as fog/smoke, to detect oncoming aircraft and provide the ability for successful avoidance?

1.4 Outline

Three different experimental setups were used to address this problem. The first experiment used four microphones placed in a tetrahedron configuration. A recording was made of an aircraft flying by the four microphones and the audio used to create a direction vector pointing towards the aircraft. The second experimental setup involved using two microphones traveling at speeds up to 50 kilometers per hour on the ground. The microphones were modified to be able to record in high winds and withstand vibrations. The final experimental setup was to place two modified microphones on an aircraft and record a sound source (model aircraft engine) on the ground.

1.5 Challenges

Many challenges were encountered throughout this thesis. One of the most challenging was wind noise. While wind socks designed to reduce wind noise are available to buy, they are not aerodynamic and will result in high wind noise when moving at high speeds. Another challenge was the self noise produced by the engine/motor of the craft as well as vibrations from the aircraft.

A smaller challenge that was encountered was that a smaller aircraft could not carry a large computer.As well, recording a flying manned aircraft during an experiment was difficult as it would be hard to fly an RC aircraft nearby due to restrictions and furthermore the sound levels and distance of the aircraft would not be reliably known. One last challenge was the number of microphones that could be mounted on board the aircraft. For accurate localization, four microphones should be used. However, the four microphones should also be spaced approximately 1 foot apart to produce a reasonable resolution, creating a challenging airborne setup. This is explained further in Section 2.1.5.

Chapter 2

Background and Literature Review

2.1 Acoustic Concepts

2.1.1 Sound Propagation

Different mediums such as air and water change the propagation properties of sound. Indeed, within a particular medium, the propagation can vary, due to the composition of the medium, the temperature and wind gradients, the wind conditions as well as the ground absorption [5].

The speed of sound in a gas depends on the temperature of the gas, higher temperatures result in higher speeds of sound. Furthermore, atmospheres are often cooler at higher altitudes, resulting in sound waves being slowed at higher altitudes [5]. This effectively causes the waves to bend towards the cooler/higher altitudes. As a result, due to this bending, there are areas wherein the sound waves do not reach except through reflections by local objects or surfaces. In some cases, such as during winter and at sunset, lower temperatures occur at lower altitudes. As a result of this, the sound waves bend downwards and propagate further along the ground. Figure 2-1 demonstrates the effect [5].

Whenever there is wind present, a wind velocity gradient will be produced, since

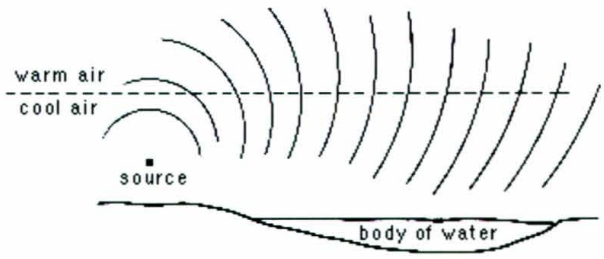

Figure 2-1: Temperature Effect on Sound Wave Propagation: sound waves bend downwards towards cooler air and propagate further along the ground [5]

the layer of air close to the ground is stationary. The resulting effect on sound propagation is that sound waves travelling upwind will refract upwards and sound waves travelling downwind will refract downwards, effectively altering the distance the sound waves traverse.

The effects of temperature and velocity gradients can cause measured sound levels to be quite different from predicted values. Depending on the conditions, the differences could be as large as 20 dB for distances of a few hundred meters [5].

Additionally, acoustic energy is also absorbed by the medium through which it traverses, known as molecular relaxation [6]. In the case of air, the amount of absorption is affected by the temperature and humidity of the atmosphere. Figure 2-2 summarizes the effects [6]. From the figure, for frequencies around 2 kHz, the absorption is typically .25 dB/100 m for 30% relative humidity and 20C. For higher frequencies, the attenuation is much greater, eg. at 8 kHz the absorption is typically on the order of 5 dB/100 m for 10% relative humidity and 20C.

On the other hand, the attenuation caused by rain, fog and snow is minimal for audible frequencies. [6]

2.1.2 Aircraft Sound

Studies have been conducted to research the noise levels produced by aircraft (including helicopters and UAS) at different distances between source and measurement [7].

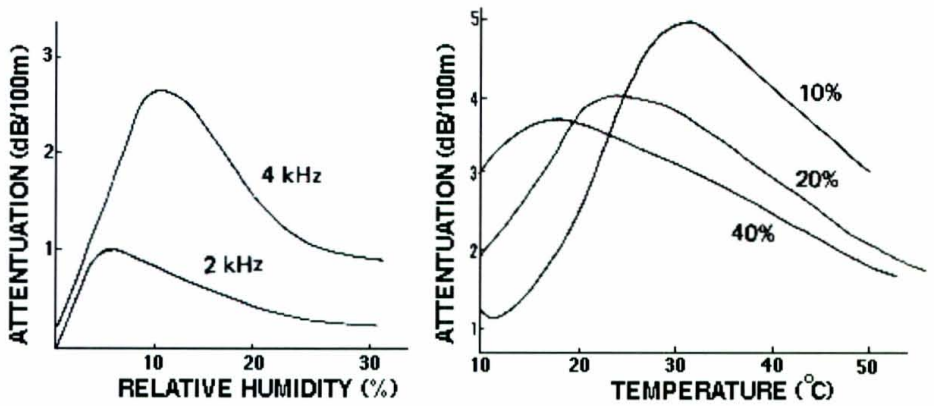

Figure 2-2: Humidity effect on absorption of sound waves ((left) Frequency dependence of attenuation as a function of relative humidity at 20C, (right) Attenuation as a function of temperature for various percentages of relative humidity (10% RH, 20% RH and 40% RH)) [6]

Table 2.1: Estimated Sound Levels for Various Aerial Craft

Distance(feet)	Helicopter Sound Levels (dBA)	Fixed Wing Craft Sound Levels (dBA)
50	97.2 to 106.7	102.2 to 110.0
1,600	64.9 to 75.0	69.5 to 71.9
3,150	57.3 to 67.6	61.1 to 63.4

Noise levels were tabulated for 10 types of aerial craft at distances ranging from 50 feet to 25,000 feet. To summarize, the Helicopters (OH-58D, UH-60, CH-47D, CH-53D, CH-53E, AH-1G and AH-1W), travelling at 100 Knots, at 50 feet produced estimated sound levels of 97.2 to 106.7 dBA. At 1,600 feet (roughly 500 meters) sound levels produced ranged from 64.9 to 75.0 dBA, and at 3,150 feet (nearly 1 kilometre) sound levels produced ranged from 57.3 to 67.6 dBA. In the case of the fixed wing aircraft (C-130, C-17 and Shadow UAV), the sound levels produced ranged from 102.2 to 110.0 dBA at 50 feet, from 69.5 to 71.9 dBA at 1,600 feet and from 61.1 to 63.4 dBA at 3,150 feet. The estimates were made using the following atmospheric conditions: Temperature 11C, relative humidity approximately 51% and average wind velocity from 6 to 9 miles per hour. These sound levels are restated in Table 2.1. Additional sound studies have been published for commercial and general aviation aircraft [8].

2.1.3 Acoustic Data Analysis

Correlation is used to measure how similar two signals are to each other. This method is used for a variety of purposes. It is used in radar, sonar, digital communication and geology applications to mention a few. For example, in radar, a signal is transmitted and then a reflected signal is received. The two signals will be similar, however the received signal will be a delayed version of the transmitted signal mixed in with additional noise. By using correlation the time delay between the two signals can be found. If the transmitted signal is contained within the received signal, the correlation will produce a peak at a particular lag or delay. This peak can be used to determine how long the signal took to travel out to an object, reflect off of of it, and return. Thus, knowing how fast the signal travels and how long it took to return, the distance to the object that the signal reflected from can be calculated.

Cross Correlation is given by equation 2.1

$$r_{xy}(l) = \sum_{n=-\infty}^{\infty} x(n)y(n-l) \tag{2.1}$$

where (l) is a time shift index or lag parameter, and where $x(n)$ and $y(n)$ are the first and second signals respecitvely.

2.1.4 Fourier Transform

To analyze a signal it is sometimes easier to convert the signal from a time representation to a frequency representation. This is achieved by applying a Fourier transform to the signal of interest.

$$X(w) = \sum_{n=-\infty}^{\infty} x(n)e^{-Jwn} \tag{2.2}$$

where capital $X(w)$ is the frequency domain representation of the signal and lower case $x(n)$ is the time domain representation of the signal.

The Fast Fourier Transform (FFT) is used extensively and is an efficient method

to calculate the Fourier Transform of a signal of interest. This method reduces computationally expensive multiplications necessary for a discreet Fourier transform into successively smaller calculations. It achieves this by decimating the signal successively until what remain is only a 2 point Fourier transform. After computing this level, the result is used to compute the next level (which also becomes a 2 point Fourier transform). This method is repeated until the whole Fourier transform has been calculated. Throughout the whole method only multiple 2 point Fourier transforms needed to be calculated reducing the number of calculations from the order of N^2 to $N * log(N)$.

2.1.5 Sound Source Localization

One method for acoustic sound source localization uses the phase of peak frequencies detected to calculate the direction of arrival of a sound's source. The basic principle involves an array of microphones, detecting one frequency of interest of one of the signals captured by one microphone of the array, and subsequently calculating the phase of the detected frequency at one moment in time. At the same moment, the same frequency should be detected by a second microphone in the array, for which its phase is calculated. By calculating the phase difference and knowing how far apart the two microphones are, it is possible to calculate the direction of arrival of the sound's source. The geometry of the problem is shown in Figure 2-3. Given that $\Delta t = t_1 - t_2$, the angle of incidence (θ) carries the relationships in Equations 2.3 and 2.4, where c is the speed of sound through the respective medium, L is the baseline distance between the two microphones and $\Delta\phi_1$ and $\Delta\phi_2$ the phase difference found by the two respective microphones [9].

$$\Delta t = \frac{L}{c} sin\theta \tag{2.3}$$

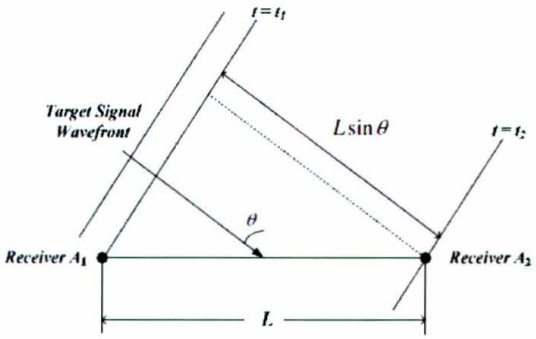

Figure 2-3: Incident Wave Geometry [9]

$$\Delta t = \frac{\Delta\phi}{2\pi f_0} = \frac{\Delta\phi_1 - \Delta\phi_2}{2\pi f_0} \tag{2.4}$$

Combining Equations 2.3 and 2.4, results in an estimate for the angle of incidence of the sound wave, for a given wavelength (λ), shown in Equation 2.5.

$$\hat{\theta} = sin^{-1}\left(\frac{\lambda}{2\pi L}\Delta\hat{\phi}\right) = sin^{-1}\left(\frac{\lambda}{2\pi L}(\Delta\hat{\phi_1} - \Delta\hat{\phi_2})\right) \tag{2.5}$$

With this relation, it is possible to localize a sound source's angle of incidence, if the assumption is made that the sound source and the microphones are co-planar. The case where the sound source is localized in 3D space is discussed in subsequent Section 3.1.

There are a few challenges involved with this method. The first challenge is that for fast moving objects, the frequencies detected by both microphones at instantaneous points in time are not the same. This is due to the Doppler shift of frequencies caused by the different relative motion of the microphones and the moving sound source. Furthermore, the microphones must be placed within a range of spacing so as to be able to calculate the phase difference correctly and avoid the problem of aliasing. Aliasing is a phenomenon where a waveform that traverses a distance of $d+2\pi$ is indistinguishable from a waveform only travelling distance d (the phase angles calculated will be identical). As a result, the microphones must be separated such

that they are not too far apart to be affected by aliasing(which is dependent on the frequency of interest being detected), yet not too close together to reduce the ability to resolve the angle of incidence of the waveform. The longer the baseline distance between the two microphones, the more accurately the angle of incidence can be estimated. Moreover, as with all methods of sound source localization this method is susceptible to noise and environmental fluctuations. If the recording of the frequencies of interest contains noise, the ability of the method to accurately localize the sound source is diminished, since the phase angles calculated are affected by the noise. This leads to another limitation of this method. If two similar frequency sound sources exist in the environment, the waveforms overlap, corrupting the phase calculation. Since aircraft produce similar frequency sound, unless the sound produced by the aircraft contains particular identifying characteristics, this method is limited to localization of only one sound source.

Another method for sound source localization is estimation of sound source direction based on sound intensity. As sound propagates through a medium, the sound pressure, measured in decibels (dB), is inversely proportional to the distance (D measured in meters) from the sound source, or $\frac{1}{D}$ [10]. Sound intensity, measured in watts per square meter, is inversely proportional to the square of the distance, or $\frac{1}{D^2}$. Knowing this, by calibrating a pair of microphones and measuring the sound pressure received by each of the microphones, it is possible to get a general sense of the direction of a sound source [11]. The microphone closest to the sound source receives more sound pressure, while the microphone further away receives a more attenuated sound pressure. The difficulty in using this technique is the requirement of many microphones to produce an accurate direction. Furthermore, if more than one sound source is present, it becomes impossible to distinguish between the two sources [10].

A third method for acoustic localization is cross correlation of the audio signals, given by Equation 3.1. Following is a description of this method. An acoustic array is used to record a segment of audio of a moving sound source. The microphones in the

array are placed in physically separate locations and along independent axes. The audio is then segmented into sections of a few milliseconds. For these audio segments, the cross correlation is found as described by Equation 3.3, a normalized version of Equation 3.1. A single recorded signal, common to both microphones, will produce a peak in the cross correlation. Due to the different physical microphone locations, an audio signal will reach the two microphones at different times. Consequently, a resulting peak will occur at a time value equal to the time delay of the audio signal source reaching the microphones. By finding this peak it is possible to find the angle of arrival of the audio signal. Furthermore, if multiple sound sources exist, they will appear as subsequent peaks in the cross correlation output [11]. This method uses the entire recording to calculate the phase difference, or time of arrival, where as the first method mentioned in this section only uses detected peak frequencies.

The use of cross correlation also applies to multi-path signals, where a single source's audio signal reaches the microphone after traversing two separate paths, which occurs when the audio array is close to the ground. The source's audio signal will reach the microphone by travelling straight to it, as well as after reflecting off the ground. These reflections will appear as secondary peaks in the cross correlation output. This method can be used with 4 microphones to find the direction of a sound in 3D space, and is able to localize multiple sound sources which is a significant advantage over the previous two methods described. Furthermore, since cross correlation is a method used to find the commonalities between two different signals it inherently deals with the noise present in the signals and discards it. More advanced techniques are available to localize a sound source using only 3 microphones, by combining energy intensity methods and cross correlation. However this is not the focus of this thesis and will be left for the reader to pursue at their own interest [12].

Application to Aircraft Localization

The cross correlation, cross spectral phase, and intensity methods discussed in the previous section were applied to aircraft localization [10]. The purpose of the project was to be able to locate aircraft which have produced a level of sound exceeding a threshold sound level over and above existing environmental noise. The application was a ground based array of microphones placed at an airport. The system was able to localize aircraft during takeoff and landing and would identify offending aircraft that exceeded the noise threshold. During the investigation it was concluded that the intensity based method could not be applied since multiple sound sources could be present at any given time; a method with higher accuracy was required. Similarly, the method of calculating the phase difference between microphones (cross spectral phase) was found to be insufficient, due to the problem that if multiple similar frequencies were present from multiple sound sources, the calculated phase of the frequency would be corrupted, leading to an incorrect direction vector. As a result, the method chosen for the application of aircraft localization was the cross correlation method as this method is able to distinguish between multiple sound sources [10].

2.1.6 Target Detection

Various methods also exist for detecting the presence of a sound source and recording it with a microphone, however these methods do not calculate the direction or location of the sound. As opposed to the localization algorithms, the methods of detection described only require the use of a single microphone. Some of the popular methods include: Log Sum, Harmonic Set and Maximum Power detectors. The log sum detector functions by branching the microphone signal into two. One of the branches is filtered by a low pass filter, the other by a high pass filter. Following, the filter outputs are logarithmically integrated over short periods of time, then compared. If the value of the high pass filter is greater than that of the low pass filter then a target signal is stated to have been detected [13].

The harmonic set detector analyzes the signal in the frequency domain. This detection method works by finding peak frequencies which are harmonically related to each other. Harmonics occur due to the sound source's rotating components. This is especially true for aircraft which operate with propellers and jet turbines. This method works by finding frequencies of interest, which are chosen by selecting separate spectral peaks. Following, the frequencies are tested to find out if two or more of the frequencies are integer multiples of a reference frequency. In most cases the reference frequency is the base harmonic or base frequency detected [14].

Lastly, the maximum power detector operates by splitting the signal in the frequency domain into clusters of frequencies. Following, the maximum spectral power for each cluster is found and its value is compared against a threshold. If the spectral power exceeds the threshold then a target signal is stated as detected [13].

Application to Aircraft Detection

The Log Sum, Harmonic Set and Maximum Power detection methods were applied and compared for aircraft detection in [13]. Each method was run on the same sets of data to obtain an understanding for how the methods compare in the categories of: probability of detection against target range as well as detection time and the probability of false alarm. The resulting conclusion inin [13] was that the Harmonic sum detector was able to perform best in spite of variations in background noise. It had a 5% false detection rate and a 98% detection rate. As well, it was able to detect turbo prop aircraft at a range of 3000 meters.

2.1.7 Improvements in Microphone Technology

To mechanically improve the performance of detection and localization algorithms, a few technologies exist. One such technology are wind socks or wind shields placed over the microphone to buffer the wind noise such that it is not received by the microphone capsule. The device improves the signal to noise ratio by decreasing the

wind noise received by the microphone while still allowing the signal of interest to pass through. An example of such is the Rycote and Rode Blimps, with additional add-ons such as the WindJammer. These devices are advertised to provide 18dB wind noise attenuation, with an additional 18dB attenuation through use of the add-on [15].

Another development over the conventional microphone is the creation of the Microflown® acoustic sensor [16]. This device differs from a conventional pressure microphone in that it measures particle velocity rather than impinging pressure; as such these devices are also named particle velocity sensors. In essence these devices are very sensitive thermal mass flow sensors, which operate by measuring minute changes in temperature between two closely spaced parallel wires. The temperature difference measured by the wires is proportional to the acoustic particle velocity. However, with only one pair of wires, the particle velocity can only be measured along one axis. To measure acoustic particle velocity in all directions, a 3D probe is used, shown in Figure 2-4 [16]. This probe is comprised of 3 pairs of wires placed orthogonally, as well as a conventional microphone capsule, which is used for calibration and amplitude measurement [17]. The size required for this acoustic localization device provides a significant advantage. Since the velocity sensors only detect sound waves perpendicular to each one's axis, the 3D sensor localizes sound by finding the direction which maximizes the particle velocity between the three velocity sensors. As a result, the probe need only be the size of the 3 velocity sensors and their required capsule, as opposed to the space required for the localization of conventional microphones, which requires the microphones to be separated by a minimum baseline distance to be able to resolve the direction of the sound source. As this sensor measures temperature differences between to wires, this leads to problems when used in high wind conditions, such as on an aircraft. The air flowing over the sensor would change the temperature of the wires and thus the reading.

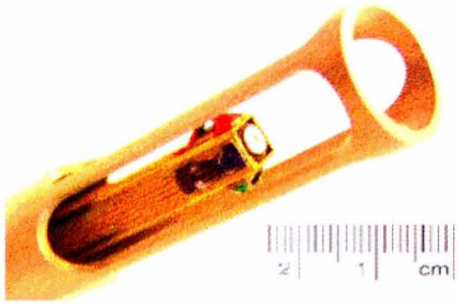

Figure 2-4: Acoustic Velocity Sensor [16]

Application to Aircraft Localization and Detection

The application of the Microflown® device is likely an interesting development towards sense and avoid systems. The research company in fact has begun testing the device for purposes of sense and avoid conducted aboard a UAS, shown in Figure 2-5 (b). Several different experiments have been conducted to test the performance of the device on board a UAS. One experiment conducted involved flying a UAS alongside a Cessna 172 Skyhawk. The result of this preliminary experiment was that the on board system was able to detect and localize the Cessna 6 seconds prior to the closest passing distance when travelling at a relative speed of 65 meters per second. The device was also shown to provide 360 degree sensing capability and an expected sound localization error of less than 0.6 of a degree [16].

Another group working on sense and avoid for unmanned aerial systems is SARA Inc. who have developed the Passive Acoustic Non-Cooperative Collision Alert System (PANCAS), an acoustic sense and avoid system, shown in Figure 2-5 (a). The system listens for low frequency sounds, between 20 and 200 Hz, and by localizing the sound using an on board computer, and analyzing the bearing and azimuth information of the sound determines if the oncoming aircraft is on a collision course with the UAS. Few details are available for this system, however it advertises up to 2 mile detection ranges [18].

(a) SARA - LOSAS [19]

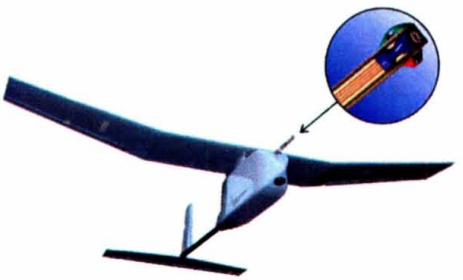

(b) Microflown Particle Velocity Sensor [16]

Figure 2-5: Acoustic Sense and Avoid Systems

2.2 Fluid Dynamics

2.2.1 Laminar and turbulent flow

To reduce the amount of wind noise affecting the microphone capsules used in the experiments described in Section 3.4.1, fluid dynamics was used to design a capsule which provided laminar airflow around the capsule. Laminar and turbulent flow are differentiated by a critical or threshold Reynolds number. When the threshold is exceeded, the fluid flow becomes turbulent which is characterized by rapid fluctuations spontaneously being established in the velocity of the fluid. Conversely, flows below the Reynolds number threshold are laminar flows and are characterized by smooth streamlines [20].

Reynolds number is a dimensionless number which is a ratio of inertial forces versus viscous forces. It is given by equation 2.6

$$Re = \left(\frac{\rho v L}{\mu}\right) \tag{2.6}$$

where v (m/s) is the relative mean velocity of the object to the fluid, μ (kg/(m $\cdot$ s)) is the dynamic viscosity of the fluid, ρ (kg/m^3) is the density of the fluid and L (meters) is a characteristic linear length given by the type of situation analyzed.

2.2.2 NACA airfoil design

NACA airfoils are designed using characteristic properties to achieve different aerodynamic performances. These airfoils were studied to improve the laminar flow of air over microphone capsules. This is explained further in Section 3.4.1. The first families of NACA airfoils developed were the 4 and 5 digit series. These airfoils were derived geometrically and before their inception, airfoil design was primarily based on experience rather than analytics. Following, the 1 or 16 series airfoils were developed, these were designed using airfoil theory as opposed to geometrical relationships [21, 22].

Chapter 3

Design of the Airborne Payload

3.1 Tetrahedron Method

Three methods that may be used for acoustic localization are analysis of sound intensity, the use of cross spectral functions and cross correlation. The first two methods will be described briefly, including the reasons they were not used; the cross correlation method will be described in more detail.

As mentioned in Section 2.1.5 sound intensity, measured in watts per square meter, is inversely proportional to the square of the distance, or $\frac{1}{D^2}$. By calibrating a pair of microphones and measuring the sound pressure received by each of the microphones, it is possible to get a general sense of direction of a sound source [11]. A microphone closer to the sound source receives higher sound pressure, while the sound pressure received by a microphone further away is more attenuated. Multiple microphones are required to produce an accurate localization and furthermore, if more than one sound source is present, it becomes impossible to distinguish between the two sources. An example of this method being used for aircraft detection is [10].

A second method for acoustic localization is the use of cross spectral functions. When comparing recordings from two microphones which are located in spatially distinct locations, a sound source will arrive at one microphone at a different time than

the other (except in the case where the sound source is located at an equal distance from both microphones). This time difference in the time-domain corresponds to a phase shift in the frequency domain. By finding the phase difference between the two recorded signals it is possible to calculate the time difference of arrival [11]. However, as with the sound intensity measurement method, if more than one sound source is recorded, it becomes difficult/impossible to distinguish between the two sources since each additional sound source corrupts/interferes with the others.

Due to these shortcomings, the method chosen for acoustic localization was that of phase correlation of the audio signals, given by Matlab Equation 3.1. Phase correlation is similar to cross correlation, however while analyzing the recorded data, this method was found to give better results and was more robust, an example is shown in Figure 3-1. Phase correlation is based on the principle that a delay in the time domain is equivalent to phase shift in the frequency domain. It factors out the signal amplitude and depends only on the phase by normalizing the magnitudes of each frequency component in the frequency domain. The resulting inverse Fourier transform will produce sharp peaks at a particular time delay where a correlation in the two signals occurs.

$$\text{Phase Correlation} = \text{fftshift}\left(\text{ifft}(\text{fft}(x).*\text{conj}(\text{fft}(y)))\right) \tag{3.1}$$

fftshift shifts the output such that array is centred around zero. fft and ifft are the Fourier and inverse Fourier transforms respectively. x and y are the two signals being compared and conj is the complex conjugate of the signal.

Following is a description of the procedure using this method. After recording a segment of audio of an aircraft flying by an acoustic array, the audio is segmented into sections of a few milliseconds. For these audio segments, the phase correlation is found as described by the Matlab Equation 3.3, a normalized version of Equation 3.1. A single recorded signal, common to both microphones will produce a peak in the phase correlation. Due to the different physical microphone locations, an audio signal

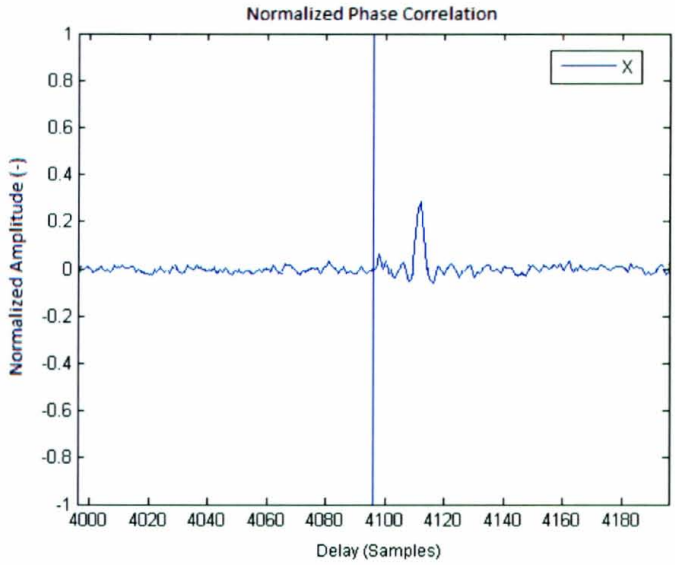

Figure 3-1: Normalized Phase Correlation: Shows the correlation one pair of microphones, the peak corresponds to the point of highest correlation between the two microphone signals being compared, and the time delay of arrival of the audio signal. (The delay in samples can be converted to seconds by dividing the delay by the sampling rate of the recording (44100 Hz))

will reach the two microphones at different times. Consequently, a resulting peak will occur at a time value equal to the time delay of the audio signal source reaching the microphones, an example is shown in Figure 3-1. By finding this peak it is possible to find the angle of arrival of the audio signal. Furthermore, if multiple sound sources exist, they will appear as subsequent peaks in the phase correlation output [11]. The use of phase correlation also applies to multi-path signals, where a single source's audio signal reaches the microphone after traversing two separate paths, which occurs when the audio array is close to the ground. The source's audio signal will reach the microphone by traveling straight to it, as well as after reflecting off of the ground. These reflections will appear as secondary peaks in the phase correlation output. At times the direct path can be obstructed and the reflected path is the signal received.

The phase correlation is found for three microphone pairs, each located in different spatial locations. As a result, a time delay value is found for the single signal from the

same source picked up by the three microphone pairs. Each delay value corresponds to a hyperbolic cone (given by Equation 3.2 where $a = b$) with an origin at the centre between the two microphones. (Note: the hyperboloid is approximated to a cone for large distances to the sound source, appropriate for aircraft localization). This means that if only one pair is used, the direction of the sound source will be ambiguous. (Note: If the sound source were assumed to be co-planar with the two microphones, the ambiguity can be reduced to either in front or behind the microphones.) By introducing a second microphone pair, a second cone is created. As such, the the source originates from locations given by the intersections of the 2 cones and the ambiguity is reduced. By utilizing three microphone pairs the ambiguity is removed and the single direction of the sound source can be identified. By using three pairs, following the computation of the peak in the phase correlation, Equations 3.4 and 3.5 can be used to find the audio source's XY plane direction and azimuth respectively [10].

$$-\frac{x^2}{a^2} - \frac{y^2}{b^2} + \frac{z^2}{c^2} = 1 \tag{3.2}$$

$$\text{xCorrX} = \text{fftshift}\left(\text{real}\left(\text{ifft}\left(\frac{\text{conj}(\text{fft}(mic_x)).*\text{fft}(mic_{zero})}{(\text{abs}(\text{fft}(mic_x)) + 1*(10^{-16})).*\text{abs}(\text{fft}(mic_{zero}))}\right)\right)\right) \tag{3.3}$$

$$\theta = tan^{-1}\left(\frac{\tau_y}{\tau_x}\right) \tag{3.4}$$

$$\phi = tan^{-1}\left(\frac{\tau_z}{\sqrt{{\tau_x}^2 + {\tau_y}^2}}\right) \tag{3.5}$$

All the variables used in the analysis are tabulated in Table 3.1.

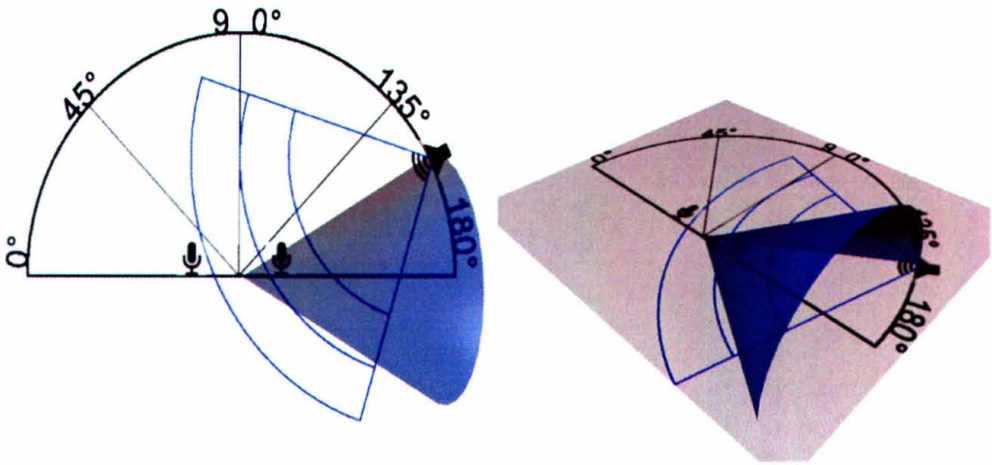

(a) Angle of Arrival on a 2D Plane (b) Angle of Arrival in 3D Space

Figure 3-2: Localization Cone: The peak from the phase correlation is used to find the delay of arrival and subsequently the angle of arrival of a sound source between two microphones. Using only one pair of microphones this angle of arrival is ambiguous in 3D space as shown in Figure B above.

Table 3.1: Variable descriptions and units

Variable	Description	Units
τ	Time Delay Between Microphones	milliseconds
θ	XY Plane Direction	Deg.
ϕ	Azimuth Direction	Deg.
mic_{zero}	Microphone Placed at Origin	Audio Recording
mic_x	Microphone Placed on X Axis	Audio Recording

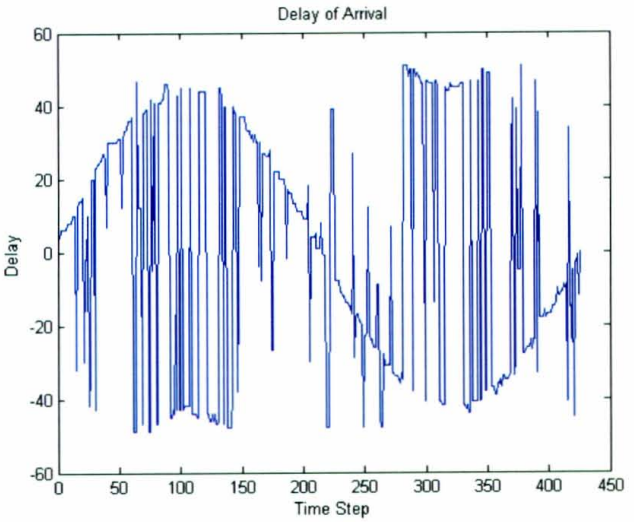

Figure 3-3: Minimum Signal to Noise Ratio: Noise levels reach a level where the original signal is lost

3.2 Noise Level Simulation and Signal to Noise Ratio

To obtain a sense of the capabilities and limitations of the direction of arrival algorithm developed a simulation was conducted. The objective was to find out how much noise could be introduced before the direction of arrival algorithm would no longer deliver valid results. The following outlines the simulation conducted.

- Create simulated sound source waveform(car horn and plane engine)
- Create a duplicate but delayed waveform simulating movement of sound source
- Add wind noise, at different SNR (Signal to noise ratio), to simulated sound source and delayed waveform
- Compute DOA (Direction of Arrival)
- Check if peak is detected
- If peak is clearly detected add more noise to the signal and recompute DOA
- Find limit SNR

This simulation suggests that a significant amount of noise can be introduced before the DOA algorithm ceases to detect the direction of arrival as shown in Figure 3-3. The sine wave visible in Figure 3-3, corresponds to the delay found between the two simulated audio channels; as more noise is introduced the sine wave is corrupted and the delay found is incorrect. However, it must be noted that this simulation involved the use of pure cosine waveforms as well as the use of Gaussian white noise. As a result, this simulation only describes smallest signal to noise ratio, working under the best conditions. In reality, wind noise does not have a normal distribution. Furthermore, a real audio recording contains secondary sound sources that corrupt the signal. These are also not normally distributed and cause additional noise in the phase correlation calculation.

3.3 Design Of Experiments

A Design of Experiments (DOE) approach was used in the following experiments in order to systematically approach and analyze the results of the experiment. DOE provides a methodology for analyzing the effects of various parameters on one or multiple outputs. As the number of parameters increases in an experiment the number of trial runs increases. DOE methodology provides an optimal approach to minimize the number of runs, and furthermore allows for the identification of interactions between parameters and their effect on the output [23]. For this thesis, DOE was used for the ground experiment in order to compare the effects of travelling at different speeds, altering the minimum distance from the sensor to the target and using different microphones to record the sound source. More detail is provided in Section 3.5.1.

3.4 Design of Capsule

3.4.1 Aerodynamics of Capsule

To reduce the amount of wind noise affecting the microphone capsules a new aerodynamic enclosure was built for the microphones.

To obtain good aerodynamic properties an airfoil was selected which maximized the laminar air flow over the airfoil. The airfoil selected was a NACA 16-012.

This 1-series NACA airfoil is described by the 5 digits. The second digit (6) indicates the location of least pressure to be at 60% of the length airfoil. The third digit indicates the lift coefficient (0%), while the final two digits indicate the thickness of the airfoil measured in percentage of cord length (12%) [21, 22].

This airfoil was selected since it had a laminar boundary layer for the first 80% of the profile as seen in Figure 3-4 [24] and was also symmetric around the horizontal axis.

T.U. stands for the transition from laminar to turbulent flow on the upper side of the profile while S.U. stands for the separation of the turbulent flow on the upper surface. The three plots $\delta 1, \delta 2$ and $\delta 3$, which are corresponding to: the displacement thickness of boundary layer, the momentum thickness of boundary layer and the energy thickness of boundary layer respectively.

Angle of Attack

In addition to the location where the turbulent flow begins over the airfoil, it is important to analyze the effect of the angle of attack, since the airfoil will not always be pointed directly into the wind. For this purpose a simulation was conducted using Java Foil [24], on the effect of changing the angle of attack to determine the effect on the position of the end of the laminar flow in the boundary layer. The simulation predicts that $\pm 3^o$ will still produce a laminar flow; beyond this, turbulent flow will occur on one side of the airfoil. The simulation results are shown in Figure 3-5.

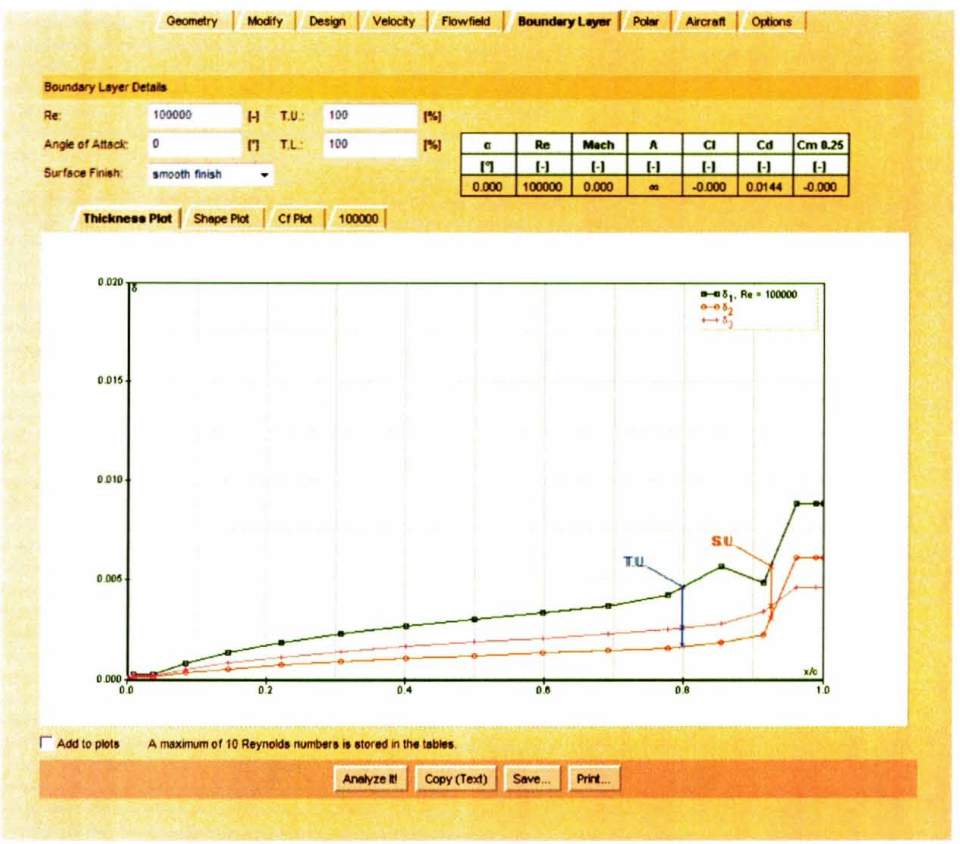

Figure 3-4: NACA 16-012 Boundary Layer Analysis: Shows the thickness of the boundary layer over the length of the airfoil profile [24]

Note that from three degrees (Figure a) to four degrees (Figure b) the position of turbulent flow on the upper side (T.U) moves from around 75% to 0%. While the aircaft is moving the capsule will point into the direction of the wind as such the $\pm$ 3^o is sufficient.

3.4.2 Manufacture of capsule

After selection of an airfoil, the coordinates were used to create a 3D model, as shown in Figure 3-6. This 3D mesh was provided to a 3D Printer/Rapid Prototype machine which printed the part using ABS Plastic, shown in Figure A.1 in Appendix A.1.

This part was then sprayed with a filler to improve the porous surface of the ABS Plastic. Following, the surface was sanded and then waxed, shown in Figure A.1. This part was then used to create two fibreglass negative molds (Figure 3-7 and Figure A.2). Using the top and bottom molds, the microphone capsule was produced, shown in Figures 3-8 and A.3.

Two different models were produced in order to compare the differences caused by using different thicknesses of fibreglass. One type of capsule was made using 3 layers of fibreglass, while a second was made using 1 layer at the nose of the capsule and 2 at the trailing end. This is explained further in Section 4.2.1.

3.5 Microphone Capsule Experiment

3.5.1 The Experiment

In order to approximate the noise level that would be present onboard the aircraft, and also to test the procedure, a ground test was designed. The ground test involved using 2 microphones spaced approximately one foot apart, recording simultaneously.

The noise inherent in these types of acoustic experiments is usually the result of three main causes. The first cause of noise is from wind. To minimize the wind noise,

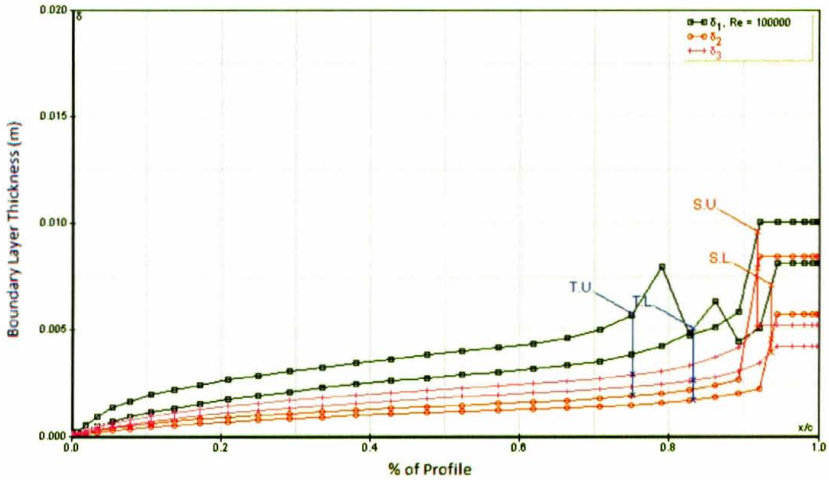

(a) Angle of Attack: 3 Degrees

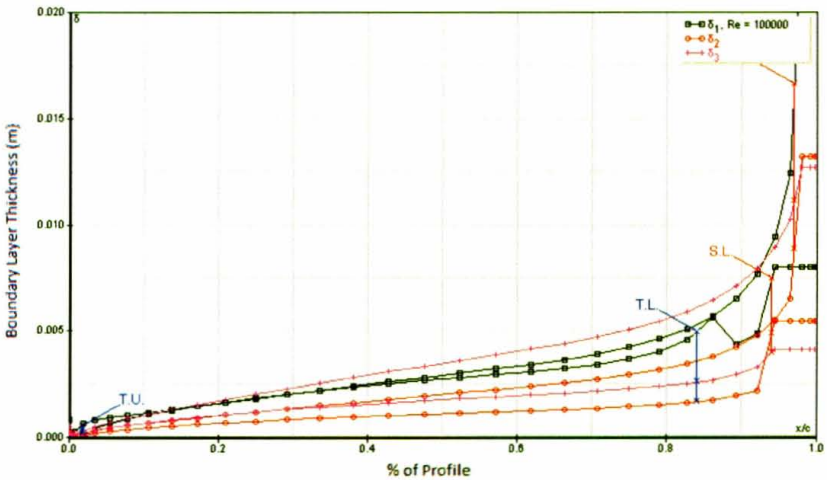

(b) Angle of Attack: 4 Degrees

Figure 3-5: NACA 16-012 Angle of Attack Analysis: As the angle of attack transitions from 3 to 4 degrees the location of turbulent flow moves from 75% of the airfoil to 0%

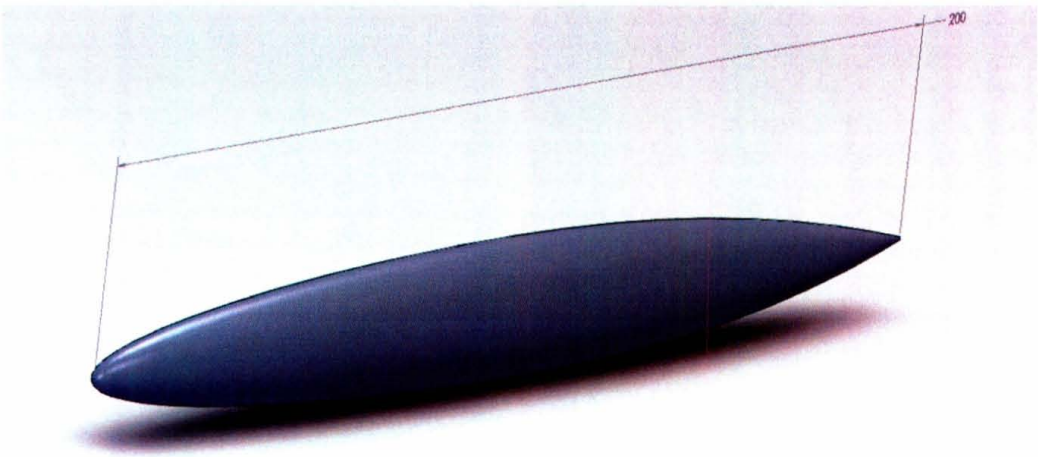

Figure 3-6: Airfoil 3D Model

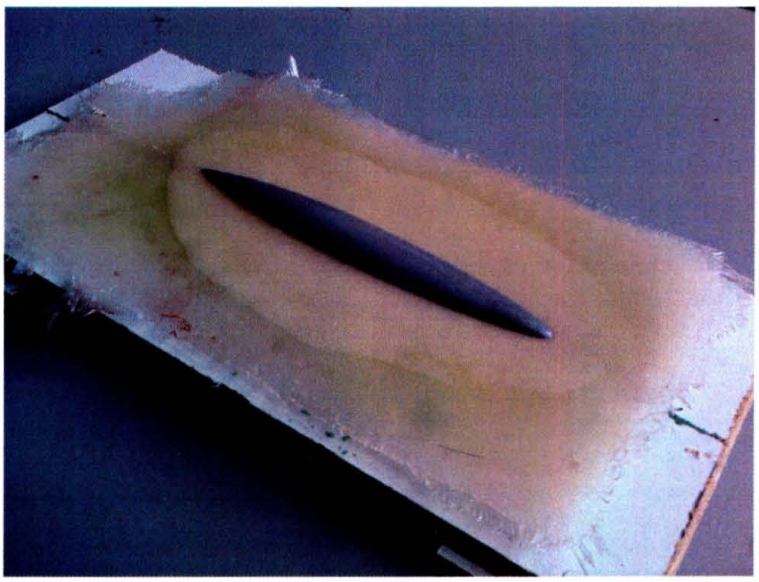

Figure 3-7: Creation of Capsule Mold

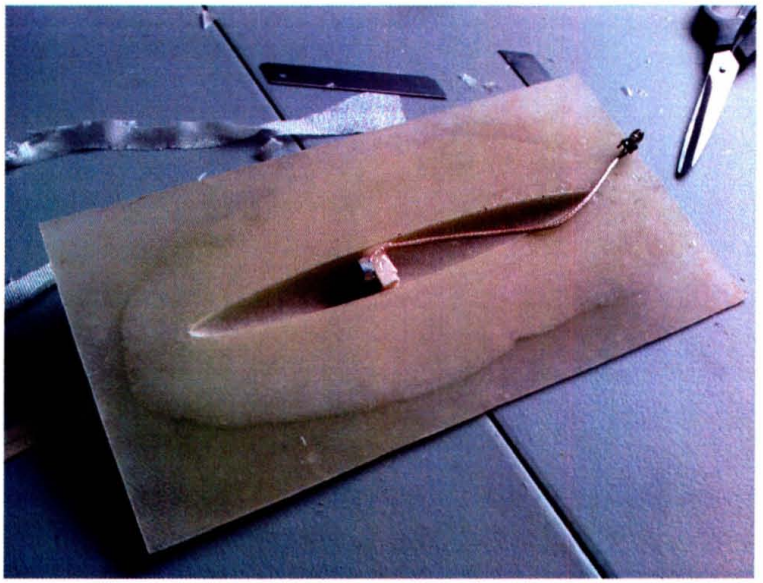

Figure 3-8: Microphone Placed inside Fiberglass Enclosure

as mentioned the microphone capsule was created to encapsulate the microphone and increase laminar flow over the microphone. A second cause for noise are vibrations from the vehicle, whether in the air or on the ground. In order to dampen these vibrations, the microphone capsule should not be connected stiffly to the vehicle. It was proposed that foam be used to absorb the vibrations so they do not reach the microphone. The last origin of noise considered was from the engine of the vehicle. In the case of the ground experiment, this would be the car's engine, tires and airflow; in the case of the air test, this would be the aircraft's motor itself, and the prop wash. To minimize this noise, the microphones are placed outside of any air flow and prop wash. Furthermore, on board the aircraft, to decrease the noise further, the motor of the craft was be momentarily ceased while on approach to the sound source.

Ground Experiment and Setup

DOE, as mentioned in Section 3.3, was used for the ground experiment in order to compare the effects of travelling at different speeds, altering the minimum distance

from the microphones to the target, and using different microphones to record the sound source. The two types of microphones used in the experiment are: the encapsulated microphone described previously and the microphone inside a GoPro camera with the water tight casing. This camera is designed for extreme sports such as skiing and surfing and includes a watertight casing, in part designed for use in high wind conditions (over 100kmph). (Note: The goPro camera contains a monophonic microphone with an automatic gain control. Additionally, the camera was tested using the open casing/baffle however the noise recorded was too high and the completely enclosing case is used.)

In order to compare the performance of the GoPro and the designed microphone capsule, as well as the effects of wind speed and minimum separation distance a DOE experiment was designed. The speed of the vehicle is varied at three different levels, 20 kmph, 40 kmph and 50 kmph. The minimum separation distance is varied from 10 meters to 20 meters, and lastly the microphones themselves were exchanged. These 3 variables create 12 possible combinations.

Airborne Experiment and Setup

Following the ground test, an air test was conducted to verify the results. In the same way that noise is minimized in the ground test, noise should be minimized for the airborne experiment. This means that vibrations from the vehicle, wind noise and engine/motor noise should be addressed. A mounting mechanism was designed for the microphones to reduce the vibrations transmitted through the airframe. Furthermore, during the experiment, the motor of the aircraft should be momentarily turned off to remove this source of noise from the recordings; in order to be able to switch off the engine/motor of the craft an electric powered craft must be used. Ideally, the flight should involve flights at various altitudes and speeds with different passing distances from the sound source.

Chapter 4

Data and Analysis

4.1 Localization Experiment

4.1.1 Tetrahedron Data

The audio signal data analyzed in the experiment was recorded using all four channels of a four channel audio recorder. The entire recording was 11 minutes long containing the audio signals of multiple flybys, of which only one, the clearest and longest, flyby was selected for the analysis. The recording was conducted on a day with relatively little wind noise, ie. wind speeds of approximately 10 knots or less. The signal to be recorded was from a Giant Big Stick, a gasoline engine powered aircraft, flying within an approximate speed range of 40 to 50 knots and at an altitude ranging between 200 and 300 feet. The engine used was a 2 stroke single cylinder gasoline engine.

Reviewing the recording itself, it is possible to note the existence of noise frequencies around 100 Hz and below, as well as a constant frequency around 210 Hz (seen in Figure 4-2), which results from a ground based electricity generator. A second harmonic of the electricity generator is also detectable in the Spectrogram at around 420 Hz. The harmonics of the aircraft become very useful in the analysis as the base frequency of the engine (around 150 Hz) is hidden by noise. Being able to detect the

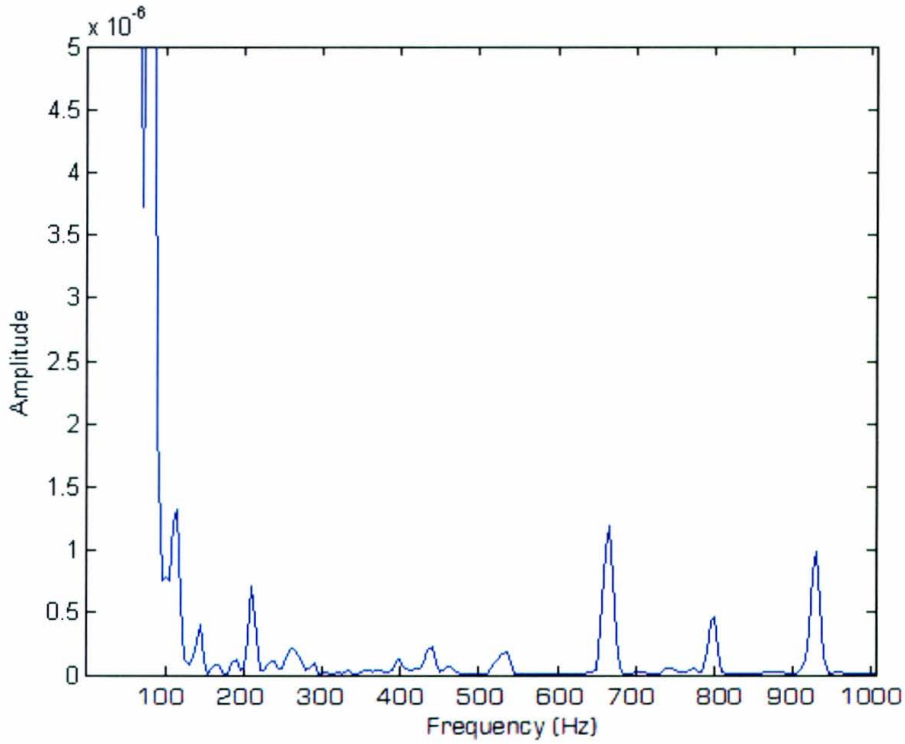

Figure 4-1: Detected Frequencies at one point in time. These frequency peaks are found for a series of time points, all of these time points together form Figure 4-2

higher harmonics allows the phase correlation analysis to be completed.

Figure 4-2 is a frequency domain representation of the audio recording. This spectrogram is generated by calculating the Fast Fourier Transform (FFT) of the signal at points in time, which reveals the frequencies present at that point in time. Calculating the FFT for a series of points in time and plotting them side by side produces Figure 4-2.

In regards to the actual audio signal emitted by the aircraft, in Figure 4-2 these are detected by the various harmonics visible, each with an approximate separation of 150 Hz (an integer multiple of the base harmonic frequency). These harmonics are an integer multiple of a base frequency at approximately 150 Hz, which is surrounded by wind and other noise. These harmonics range from the base frequency of 150 Hz

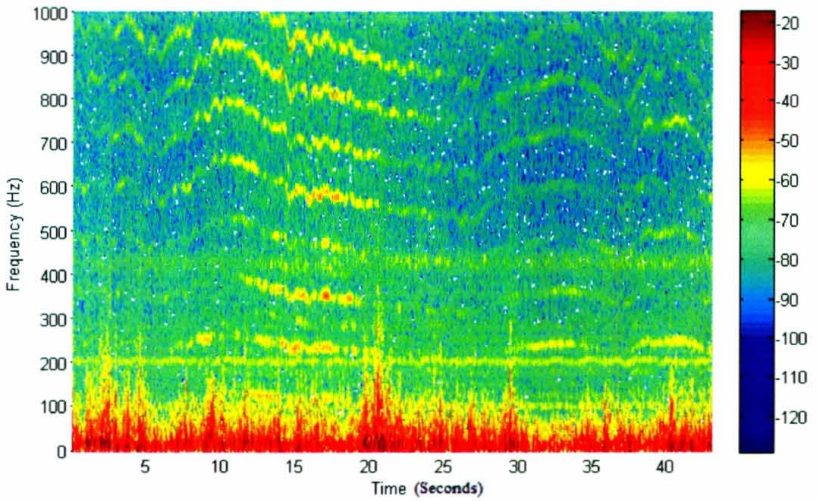

Figure 4-2: Spectrogram of Recorded Flyby: Closest approach occurs at 17 seconds. The entire aircraft flyby starts at 10 seconds and ends at 25 seconds

to approximately 1.5 KHz in Figure 4-2. This spectrogram was produced by dividing the signal into windows, each containing 4096 samples, where the sample frequency is 44.1 KHz, and where each window contains a 50 percent overlap with the adjacent windows. For each window a FFT was computed, shown in Figure 4-1. Placing the outputs of the FFT adjacent to eachother in a time sequence allows the peaks to be visible through time, as shown in the specrogram. The colour gradient describes the relative intensity of the frequency present in the recording.

4.1.2 Tetrahedron Analysis

The time difference of arrival of a sound source's signal was calculated by first calculating the phase correlation of recordings from different microphone pairs. The phase correlation was calculated over various moments in time. Next, the output of the phase correlation was searched to identify peaks. The peaks indicate a significant correlation between the two audio signals. A peak greater than the local average can be considered a target. The location of the peaks correspond to the time delay of

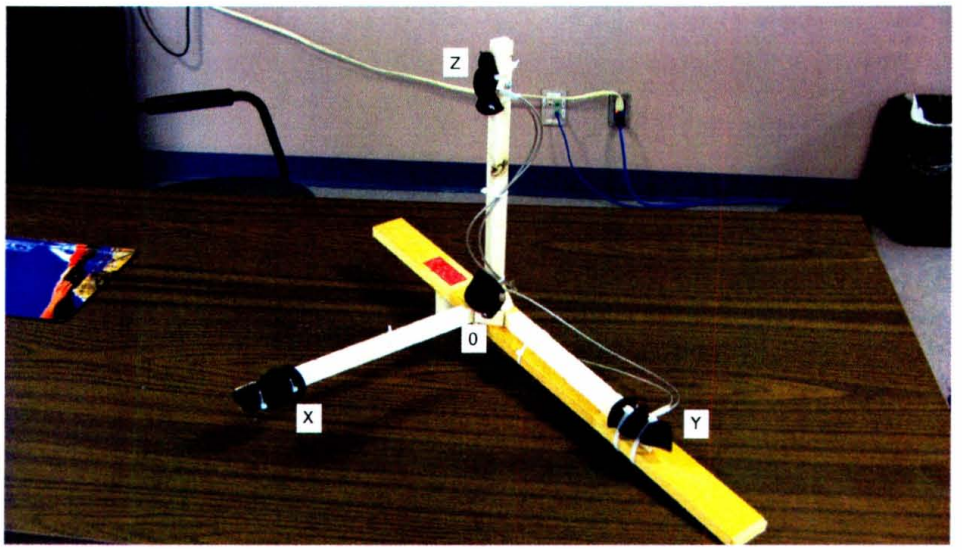

Figure 4-3: Model of Acoustic Array: 4 microphones placed orthogonally to each other used to localize a sound source. Microphone axis are labeled according X, Y and Z.

arrival of a sound signal between the microphone pairs. Using this time delay and knowledge of the locations of the microphone pairs, a direction of arrival was found. For this analysis, audio signal data was recorded using an array of microphones in the geometry described by Figure 4-3. The four microphone channels were recorded simultaneously while a gas engine powered aircraft was flown in loops at different altitudes and distances. To decrease the amount of noise from ground sound sources recorded, and to decrease the ground effects, the microphones were raised approximately 10 meters off the ground.

Since the size of the time segment is important, the first step in determining the direction of arrival was to separate the signal into time segments of a few milliseconds each. The audio frequencies of interest range from 150 Hz to 1.5 KHz. These correspond to wavelengths of 228 centimeters to 22 centimeters respectively. Consequently, to record one wavelength at these higher frequencies would require a minimum of 7 milliseconds of audio or approximately 309 samples (at 44,100 samples per second). A larger segment size of 92 milliseconds is used (4096 samples each at 44,100 sam-

ples per second) to obtain a better correlation. However, the number of samples per segment will decrease as this method moves towards real time implementation.

Next, these segments were multiplied by a Hamming windowing function to reduce edge effects and improve frequency resolution, given by Equation 4.1, where N is the width of the window. For each segment the phase correlation is found, following Equation 3.3. The microphone pairs used were: X and Zero, Y and Zero and Z and Zero, following Figure 4-3. Additional pairs could be used (XY, XZ and YZ), however for this experiment the redundancy was not required. The result of this calculation for one segment is shown in Figure 4-4. The three visible peaks correspond to the high correlation found between each of the three microphone pairs. The vertical line in Figure 4-4 corresponds to the phase correlation of the two signals at zero delay. The sampling rate of the recording system is 44.1 Khz. This implies the delay in samples must be multiplied by $\frac{1000}{44100}$ to obtain the delay in milliseconds.

$$w(n) = 0.54 - 0.46 * cos\left(\frac{2\pi n}{N-1}\right) \tag{4.1}$$

For each of the segments, a peak is produced by the phase correlation. To find this peak, the entire output of the phase correlation could be searched for the largest peak. However, since each segment of audio is 4096 samples long the phase correlation output is 4096*2 - 1. This would be a lengthy search; it is possible to speed up this search by limiting the relevant output searched. The microphones used in this experiment were spaced 28 centimeters apart. Due to the speed of sound, the maximum delay that could occur between the two receiving microphones is when the audio signal is incident on the two microphones at an angle of 0 or 180 degrees. This translates to a maximum delay of approximately 1 millisecond or 50 samples. As a result, the phase correlation need only be searched from $\pm$ 50 samples of the zero delay point.

The peaks found for each segment were then stored in an array, one array for each audio pair. These are shown in Figures 5-1, 5-2 and 5-3. A trend is visible in

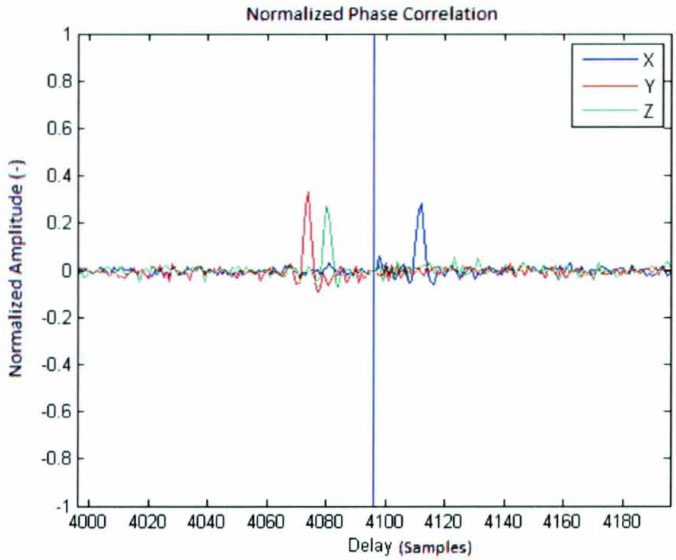

Figure 4-4: Normalized Phase Correlation: Blue corresponds to the correlation of the X axis microphones, Red to the correlation of the Y axis microphones and Green to the Z axis microphones

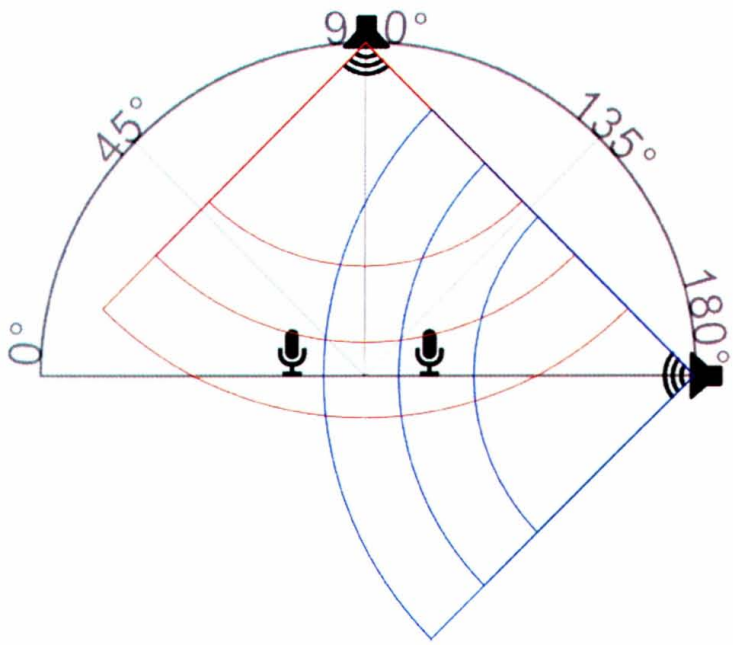

Figure 4-5: Angle of Arrival: The maximum delay of arrival between the two receiving microphones occurs when the audio signal is incident on the two microphones at an angle of 0 or 180 degrees

each of the figures. This depicts the movement of the aircraft as it moves in time. Equations 3.4 and 3.5 can be used to find the source's audio signal's XY plane direction and azimuth respectively. This 3D direction is shown in Figure 5-4. This direction is with respect to the acoustic array, with the Y-axis pointing in the general direction of the aircraft.

Pre-Processing

Recognizing the need to improve the signals output, several different measures were evaluated to improve the phase correlation result. The first measure that immediately improved the output was to remove the DC offset from each of the recordings. This was accomplished by using the 'Detrend' function in Matlab. A second measure taken was to attenuate the frequencies outside of the region of interest (150Hz to 1500Hz), however, this did not visibly improve the output of the phase correlation. This is likely due to the normalization of the phase correlation which negates the attenuation caused by the filter.

4.2 Ground Experiment

4.2.1 Frequency Response

In order to improve the recordings obtained, a microphone capsule was designed as described in Section 3.4.1. This capsule was designed to minimize the wind noise that would impinge on the microphone by creating a laminar flow of air surrounding the microphone.

Two different capsules were manufactured, the first using three layers of fibreglass throughout and the second using 1 layer for the nose of the capsule and two layers in the rear. A comparison of the two was made in order to observe the effects of using different thicknesses for the shell. Figure 4-6 shows the frequency spectrogram for the two capsules, from 0 to 10,000 Hz. The top image shows the frequency spectrogram

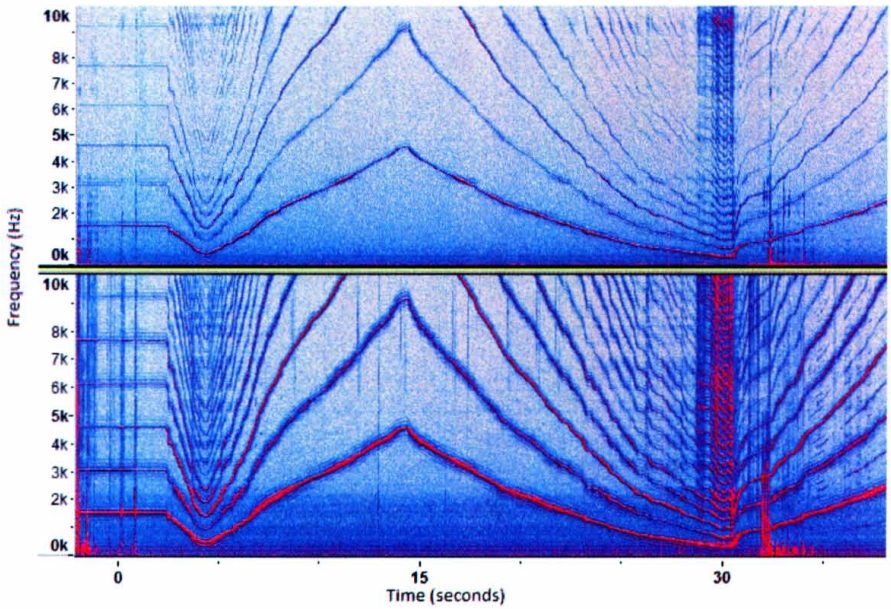

Figure 4-6: Frequency Spectrogram Comparison of Microphone Capsule Designs: (Top) Spectrogram of the recording using capsule made with three layers of fibreglass, (Bottom) Spectrogram of the recording using the capsule made with one layer of fibreglass

of the capsule with 3 layers of fibreglass, and the bottom image the spectrogram of the capsule with 1 layer. In this experiment, the capsules were used to record a set of speakers producing a variable frequency. This frequency varied from 100 Hz to 4,000 Hz. Harmonics are visible in this spectrogram. Comparing the top and bottom images, attenuation is visible between the two spectrogram. Furthermore, as shown in the frequency response in Figure 4-7, the thickness of capsule wall makes a significant difference in the attenuation of frequencies that pass through. The 3 layered fibreglass capsules attenuate sound between 20 to 30 dB more than the 1 layered capsules. For both the ground and air experiments, the one layer capsule was used.

A similar frequency response test was conducted, on a different occasion, on the goPro camera, the result is shown in Figure 4-8. The interesting pattern is caused by aliasing where compressions within the sealed case of the camera causes different

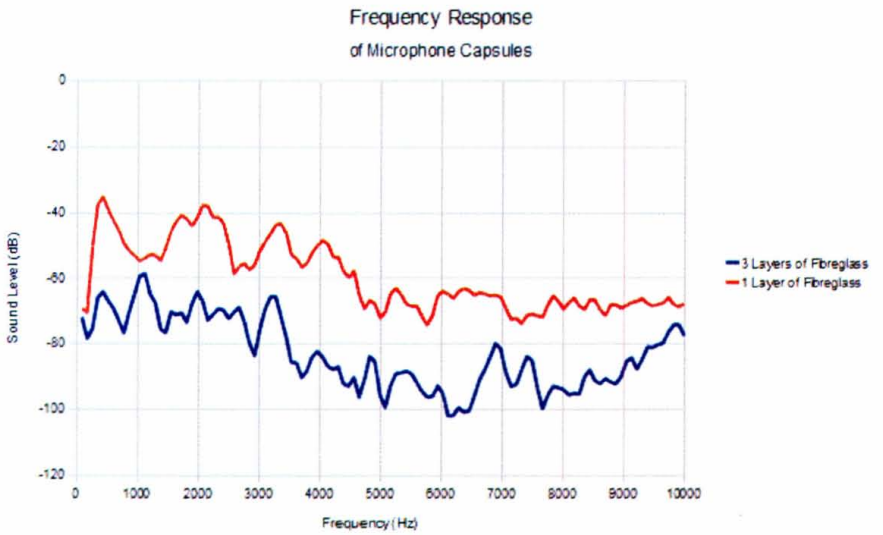

Figure 4-7: Frequency Response Comparison of Microphone Capsule Designs: The 3 layered fibreglass capsules attenuate sound between 20 to 30 dB more than the 1 layered capsules.

frequencies to constructively and destructively interfere. Furthermore, it should be noted that the goPro camera likely contains an automatic gain control which adjusts the gain of the microphone.

4.2.2 Ground Experiment Data

Taking into consideration the various sources for noise described previously(wind noise, vibrations and self engine noise), a microphone mount was created to hold the microphones outside a vehicle while driving up to 50 kilometres per hour. This setup is shown in Figure 4-10. The experiment was comprised of several trials; during each trial an audio recording from the moving microphones was made of a stationary car horn. This experiment was designed in order to compare the effects of traveling at different speeds, altering the minimum distance between the microphones and the sound source (car horn), as well the difference between the different types of microphone enclosures on the detection distance. The detection distance is based on

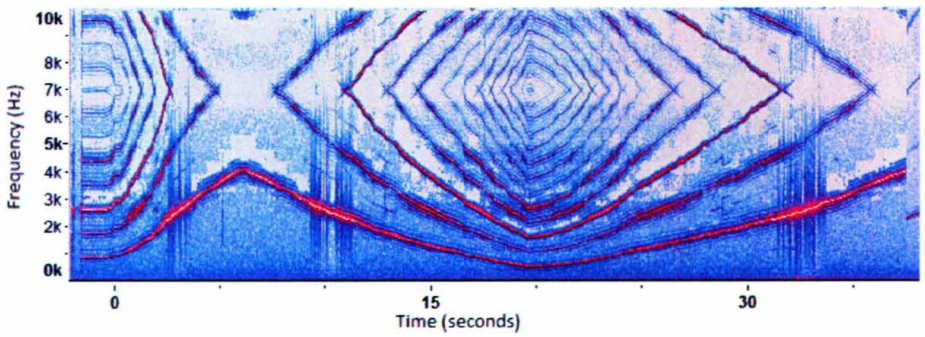

Figure 4-8: Frequency Response using the GoPro Camera

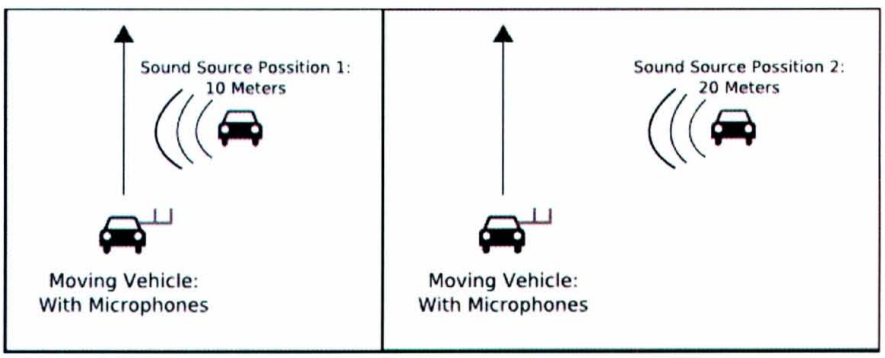

Figure 4-9: Vehicle Setup for Ground Based Test: One vehicle travels straight forward at varying speeds carrying the microphones, while a second vehicle (the sound source) is stationary by the side of the road at a distance of 10 and 20 meters.

the sound level of the car horn recorded. During each trial the following parameters were altered.

The first parameter, speed, was altered between 20, 40 and 50 kilometres per hour. The second parameter, separation, was altered between 10 and 20 meters. The last parameter, the microphone, was altered between the designed capsules and the GoPro camera with watertight enclosures. This ground experiment is depicted in Figure 4-9.

To analyze each of these parameters a total of 12 runs were conducted.

Figure 4-13 is a side by side comparison of the recordings provided by the goPro and the designed microphone capsule. Figures A.4, A.5, A.6, A.7 and A.8 in Ap-

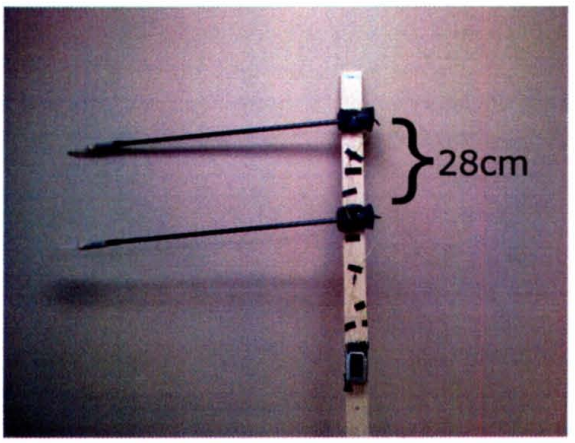

Figure 4-10: Microphone Setup for Ground Based Test: Two microphone capsules placed in parallel and plugged into an audio recorder.

Figure 4-11: Microphone Setup for Ground Based Test: Microphones are places away from the vehicle to get away from the engine noise and airflow around the vehicle.

Figure 4-12: Drive-by for Ground Based Test

pendix A.2 are comparisons for the other speeds and separations. The noise levels present in the goPro recordings are evident with the side by side comparison. The wind noise indeed masks the frequencies produced by the car horn making them much more difficult to detect. Furthermore, only at very low speeds does the goPro camera seem to perform similarly to the designed microphone capsule. The analysis in the following section will test these results to verify which parameters truly have a significant effect on the detection distances.

4.2.3 Ground Experiment Analysis

Significance of Results

The data collected in the ground experiment was analyzed using the Design of Experiments methodology previously introduced. Each of the parameters, (speed, distance and type of microphone) were tested for significance. This means that the parameters in the experiment are tested to see how their change in value affects the detection distance. Various software are available for this purpose, the one used is Design

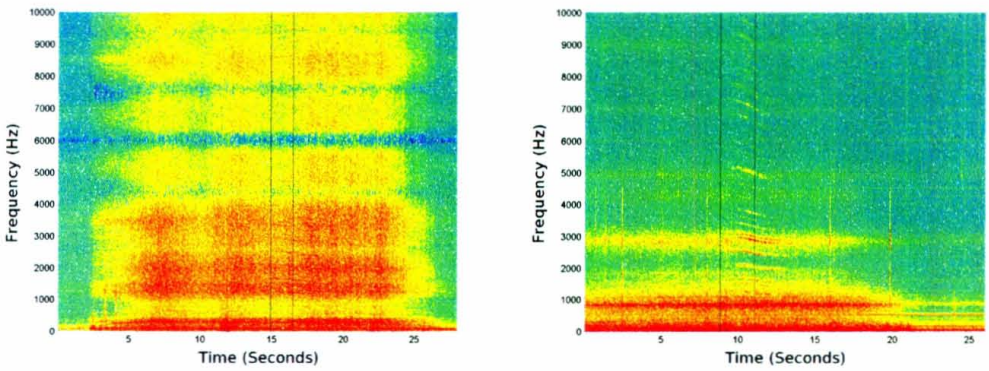

(a) goPro (b) Microphone Capsule

Figure 4-13: Spectrogram comparison of goPro and capsule at 50 kilometres per hour and 10 meter separation. First line is point of detection, second line is point of closest approach.

Table 4.1: GoPro Ground Test Results

Speed (kmph) / Distance (meters)	Detection Time (seconds)	Detection Distance (meters)
50 / 20	1.62	22.5
40 / 20	4.29	47.6
20 / 20	11.63	64.6
50 / 10	0.94	13.06
40 / 10	1.41	15.7
20 / 10	9.92	55.1

Expert. This method also allows interaction effects to be tested, which can occur when two parameters in combination affect the output in a different way than both of the parameters would individually. The detection distances for each of the trials is tabulated in Tables 4.1 and 4.2.

Through design of experiments the three parameters were tested for significance using a procedure called Analysis of Variance (ANOVA) [23]. All three main effects were found to be significant, the interaction effects were tested also but were found to be insignificant in their effect on the output. For this analysis, the following assumptions are made, independence of cases, constant variance of the data, independent measurements, normally distributed data and sparsity of effects. The ANOVA

Table 4.2: Microphone Capsule Ground Test Results

Speed (kmph) / Distance (meters)	Detection Time (seconds)	Detection Distance (meters)
50 / 20	3.652	50.72
40 / 20	7.33	81.44
20 / 20	15.576	86.53
50 / 10	2.728	37.86
40 / 10	3.918	43.53
20 / 10	11.083	61.57

analysis will show if these assumptions are correct.

Reviewing the results from Design Expert, shown in Figure 4-14, it can be seen that Factors A, B and C, (Speed, Distance and Type of Microphone), have p-values (test of statistical significance) of <0.0001, 0.0031 and 0.0026 respectively. Since these values are below 0.0500, the probability that the Null Hypothesis, (that the means are the same and that the parameter has no connection to the detection distance), is true is very low. This would suggest, therefore that all three parameters have a significant effect on the detection distances found.

The residual shown in Figure 4-14 is quite low, thus the effects not included in the model appear to have little significance. The R squared value, shown in Figure 4-15 is very close to 1 which implies a good fit. As well the adjusted R-squared and predicted R-squared values are within 0.2 of each other which suggests there is not a problem with the model. Lastly, the Adequate precision is above 4 which means there is an adequate signal to noise ratio.

Reviewing the Normal Plot of residuals from the Design Expert analysis shown in Appendix A.3 in Figure A.9, there appears to be little pattern to the deviation from the normal probability. This suggests that the data collected is normally distributed and confirms this assumption. Figure A.10 shows the plot of the Residuals vs. Predicted. The data points appear to be randomly scattered. As such there is no need for a transformation of the data, as well as confirming the assumption of constant variance. Figure A.11 shows the Residuals vs. Run plot. The data in this plot appears to be randomly scattered which suggests that there are no other factors that may be

ANOVA for selected factorial model

Analysis of variance table [Classical sum of squares - Type II]

Source	Sum of Squares	df	Mean Square	F Value	p-value Prob > F	
Model	249.49	4	62.37	73.13	< 0.0001	significant
A-Speed	*215.17*	*2*	*107.59*	*126.13*	*< 0.0001*	
B-Distance	*16.59*	*1*	*16.59*	*19.45*	*0.0031*	
C-Microphon	*17.73*	*1*	*17.73*	*20.79*	*0.0026*	
Residual	5.97	7	0.85			
Cor Total	255.46	11				

The Model F-value of 73.13 implies the model is significant. There is only a 0.01% chance that a "Model F-Value" this large could occur due to noise.

Values of "Prob > F" less than 0.0500 indicate model terms are significant.
In this case A, B, C are significant model terms.
Values greater than 0.1000 indicate the model terms are not significant.
If there are many insignificant model terms (not counting those required to support hierarchy), model reduction may improve your model.

Figure 4-14: ANOVA results

Std. Dev.	0.92	R-Squared	0.9766
Mean	6.17	Adj R-Squared	0.9633
C.V. %	14.98	Pred R-Squared	0.9313
PRESS	17.55	Adeq Precision	24.495

The "Pred R-Squared" of 0.9313 is in reasonable agreement with the "Adj R-Squared" of 0.9633.

"Adeq Precision" measures the signal to noise ratio. A ratio greater than 4 is desirable. Your ratio of 24.495 indicates an adequate signal. This model can be used to navigate the design space.

Figure 4-15: ANOVA results

Table 4.3: Cessna 182 Sound Levels

Distance (meters)	Sound Level (dBA)
6,500	70
3,250	76
1625	82
812	88
406.25	94

affecting the results, such as the measurements changing over time. Reviewing Figure A.12 the Box-Cox plot shows that the 95% confidence interval includes 1 and thus does not recommend a transform. Lastly, its not possible to test for the independence of cases, this is assumed to be true.

These results show that the use of the microphone capsule does have a significant effect on the detection time and distance of the sound source. The ground test shows that at 50 kilometres per hour the sound source can be detected at a distance of between around 35 meters and 50 meters.

Real World Equivalent

To compare these values to those that would be found in the air, the sound levels of the car must be compared to those of an aircraft. A car horn produces a sound level of approximately 88 dBA at a distance of 8 meters [25]. On the other hand a Cessna 182, (an aircraft likely to be the one encountered during UAS missions) produces a sound level of 70 dBA during takeoff at a distance of 6,500 meters [8]. For every doubling of distance there is a -6 dB drop. As such, at a distance of 3,250 meters the Cessna produces a sound level of 76 dBA. Continuing this extrapolation, at a distance of approximately 810 meters the Cessna produces a sound level of 88 dBA (shown in Table 4.3). Thus, under the same conditions and a similar microphone setup, an aircraft such as the Cessna 182 would be detected at a range of 812 meters. These values are also similar for other general aviation craft, such as a Piper or Beech. On

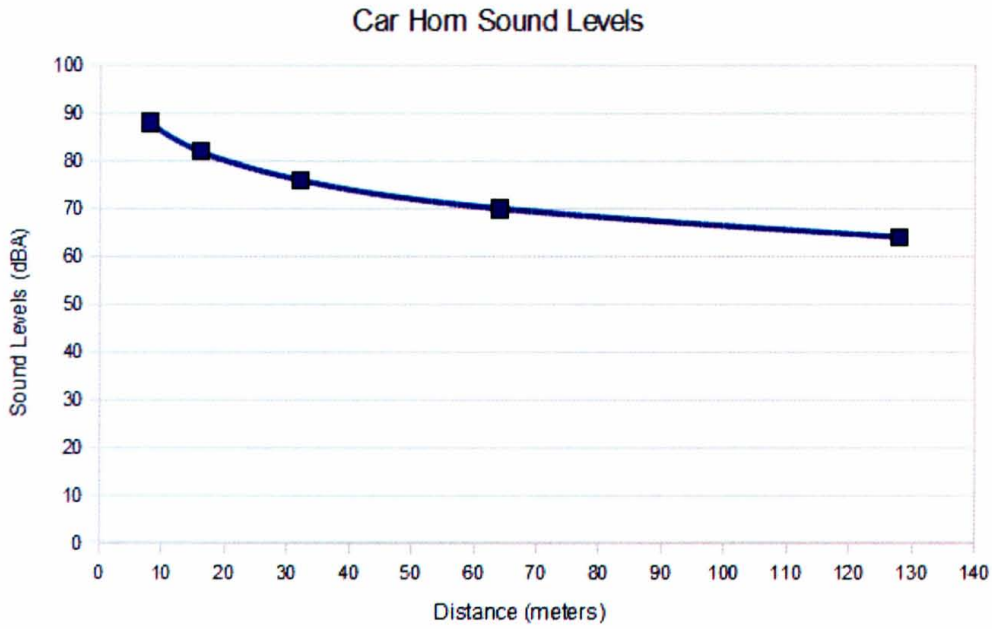

Figure 4-16: Car Horn Sound Levels: Graph shows the decrease in sound level observed as the distance from the sound source increases.

the other hand a Boeing 747 produces sound levels of 100 dBA at distance of 6,500 meters.

Expanding upon the data from Tables 4.1 and 4.2, the sound levels for each of the detected distances are added and shown in Tables 4.4 and 4.5. The sound levels for the car horn at different distances are shown in Figure 4-16 (interpolated using Equation 4.2, which is a best fit for the curve representing the decrease in sound level, where D is the distance from the sound source). Using these sound levels and the interpolated sound levels from Table 4.3 (shown in Equation 4.3, where SL is the sound level produced), the distances a Cessna produces these sound levels is shown in the last column of Tables 4.4 and 4.5. Summarizing these results, at 50 kilometers per hour the goPro would detect the Cessna at a range of 1,322 meters to 2,278 meters while at 20 kilometres per hour this range increases to 5,579 to 6,541 meters. On the other hand, the microphone capsule at 50 kilometres per hour would detect the Cessna

Table 4.4: GoPro Ground Test Analysis

Speed (kmph) / Distance (meters)	Detection Distance (meters)	Sound Level (dBA)	Cessna Equivalent Distance (meters)
50 / 20	22.5	79.04	2278.56
40 / 20	47.6	72.55	4820.42
20 / 20	64.6	69.9	6541.99
50 / 10	13.06	83.75	1322.58
40 / 10	15.7	82.15	1589.93
20 / 10	55.1	71.28	5579.94

Table 4.5: Microphone Capsule Ground Test Analysis

Speed (kmph) / Distance (meters)	Detection Distance (meters)	Sound Level (dBA)	Cessna Equivalent Distance (meters)
50 / 20	50.72	72	5136.38
40 / 20	81.44	67.9	8247.37
20 / 20	86.53	67.37	8762.83
50 / 10	37.86	74.53	3834.05
40 / 10	43.53	73.32	4408.25
20 / 10	61.57	70.32	6235.15

at a range of 3,834 meters to 5,136 meters while at 20 kilometres per hour this range increases to 6,235 to 8,762 meters, (assuming the same meteorological conditions).

$$CarHornSoundLevel = -8.66 * ln(D) + 106 \tag{4.2}$$

$$CessnaEquivalentDetectionDistance = e^{\frac{SL-145.99}{-8.66}} \tag{4.3}$$

4.3 Airborn Experiment

4.3.1 Capsule Air Data

As previously described, an air experiment was conducted to verify the results of the ground experiment. The microphones were mounted on a small electrically powered Ultra Stick airframe as shown in Figure 4-17. This aircraft was flown at various altitudes around the sound source, which for this experiment was a DLE-30, 30.5 cc, 2 stroke engine. This engine was used to replace the car horn to more closely simulate a sound source found during real operations. This engine, using the stock muffler, produces 95 dB at 2.7 meters when at maximum throttle. A GPS record was also

taken of the flight path in order to determine the maximum distance the sound source was heard from the microphones.

The two microphones were mounted on either side of the wing of the Ultra Stick, which has a wingspan of 1675mm. Each of the microphones was mounted on a boom pole in order to get the microphones out and away from the noise produced by the aircraft. This includes noise from the engine, vibrations from the airframe as well as the sound of the wind flowing over the airframe. In addition, the connection from the microphone capsules to the booms and from the booms to the wing were padded with acoustic dampening foam to reduce the vibrations that are transmitted even further.

Using an electrically powered aircraft was beneficial to the experiment, as it meant that the motor could be momentarily shut off, allowing the aircraft to glide without producing as much noise. Due to the size of the aircraft and the drag produced by the microphones the plane could only glide for 1 to 2 seconds. Nevertheless, this short time frame was sufficient to provide a window where the electric motor and propeller did not create any noise, and to sense what other noises were present.

To calculate the minimum separation between the sound source and the aircraft Equations 4.4 and 4.5 can be used, where: latDegRef and latDeg are the latitude degrees for the starting point and ending point respectively; longDegRef and longDeg are the longitude degrees for the starting point and ending point respectively and 6356752 is the radius of the earth in meters (Note: These equations are approximations, converting the lat/long positions to UTM coordinates first. produces a result that deviates less than 1%). Using these equations and the GPS data in Table 4.6, the separation along the ground is given by $\sqrt{D_x^2 + D_y^2}$, where D_x and D_y are the distances, in meters, in the x and y axis respectively, and the separation in 3D space is given by $\sqrt{D_x^2 + D_y^2 + (A_{ref} - A)^2}$, where A is the altitude, in meters, (recorded in the GPS log) at the given point and A_{ref} is the altitude at the starting point. This resulted in a ground separation of 9.47 meters and a 3D separation of 10 meters.

Figure 4-17: Acoustic Air Experiment

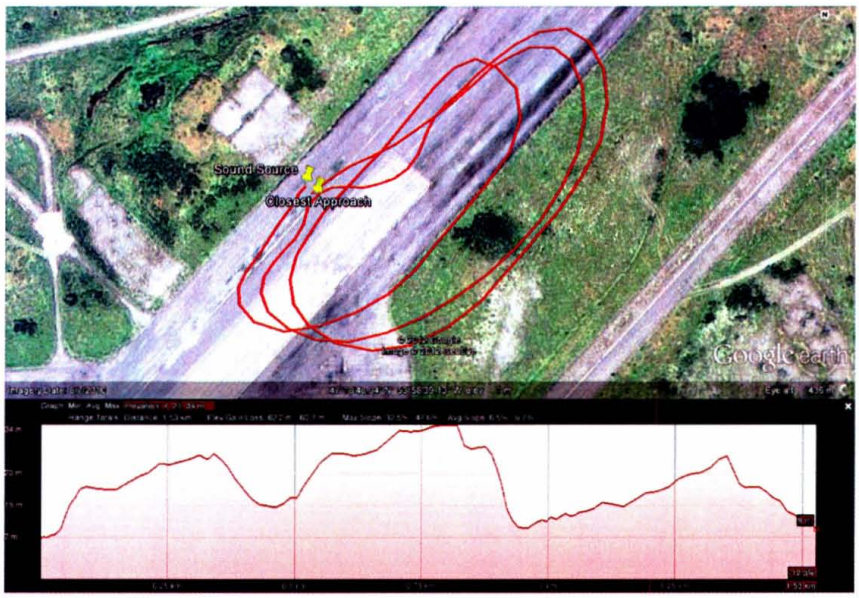

Figure 4-18: Airborne experiment flight track showing the starting point of the flight and the point of closest approach (Top) as well as the elevation profile of the flight (Bottom).

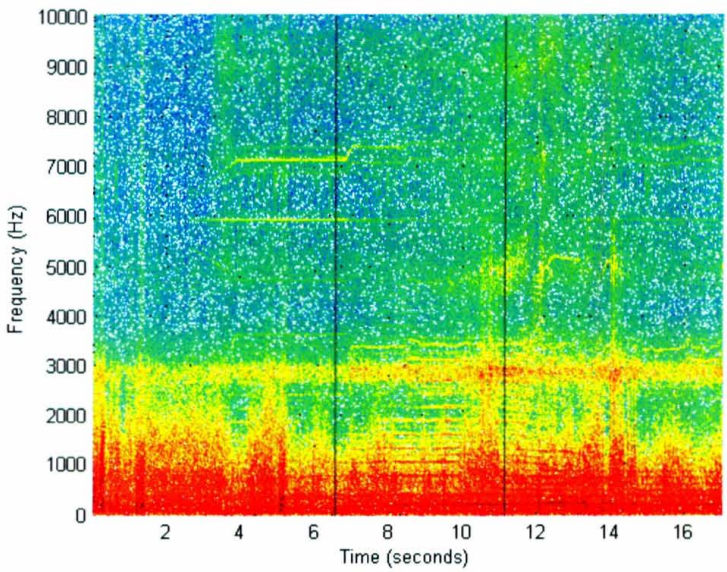

Figure 4-19: Airborne Experiment Spectrogram: Aircraft flying at approximately 32 km/h. first line represents point of detection, second line is point of closest approach.

Table 4.6: GPS Recorded Data

WNO	TOW	Time	Date	Speed	Longitude	Latitude	Altitude	Mode
1676	315911	15:44:56	2/22/2012	0	-53.981817	47.313542	7.945492	2
1676	315990	15:46:15	2/22/2012	32	-53.981710	47.313497	11.196990	2

$$D_y = (latDeg - latDeg_{ref}) * 6356752 * \frac{2 * pi}{360} \tag{4.4}$$

$$D_x = (lonDeg - lonDeg_{ref}) * 6356752 * cos\,(latDeg_{ref}) * \frac{2 * pi}{360} \tag{4.5}$$

Figure 4-19 shows the spectrogram of the audio recording for the airborne experiment. During the closest approach to the sound source, the aircraft was travelling at 32 kilometres per hour. The sound source is detected approximately 4.5 seconds before this point, resulting in an approximate detection distance of 42 meters.

Completing a similar analysis to the ground experiment, the sound levels produced by the DLE - 30 are compared to those produced by a manned aircraft. However, to do this the 95 dB from the DLE 30 must first be converted to dBA sound levels. This is achieved by taking frequencies produced by the motor, and for each of the frequencies, subtracting or adding from their respective dB soundlevels, a weighting factor. However, the sound levels are not known for each of the different frequencies. As such it is not possible to calculate precisely the dBA sound levels of the DLE - 30. However, for the frequencies of interest of the DLE - 30, the weightings that have to be subtracted are between -10 and +1 dB (shown in Figure 4-20 [26]). This results in a range of 85 dBA to 96 dBA at 2.7 meters. The more conservative value of 95 dBA will be used for the analysis.

Using this sound level the equivalent detection distance for a Cessna, as was done in Section 4.2.3, is calculated. The sound levels for the DLE 30 engine are shown in Figure 4-21. Using this graph the sounds levels are approximated for the DLE 30 at 40 meters. Next, the Cessna equivalent distance for that sound level is found using

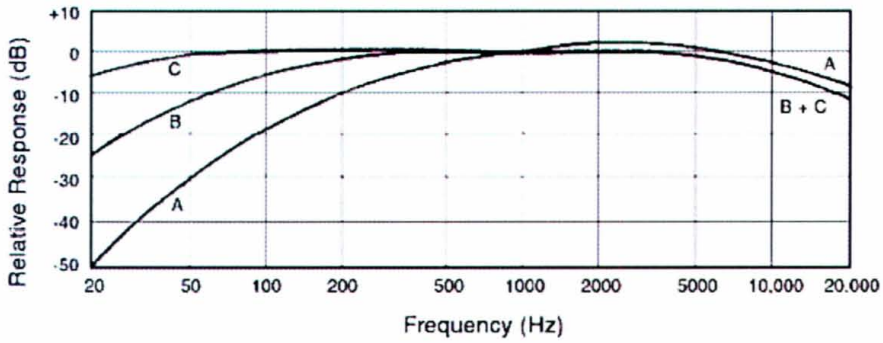

Figure 4-20: Acoustic Weighting Curves [26]

Equation 4.3. The sound level for the DLE 30 at 40 meters is approximately 73 dBA, at this sound level the Cessna is approximated to be at a distance of 4761 meters. Comparing the DLE 30 sound levels to those recorded by Stryker Brigade Combat Team [7], a Shadow UAV produced 71 dBA at a distance of nearly 500 meters. Thus it is expected that a Shadow UAV would be detected when approximately 500 meters away.

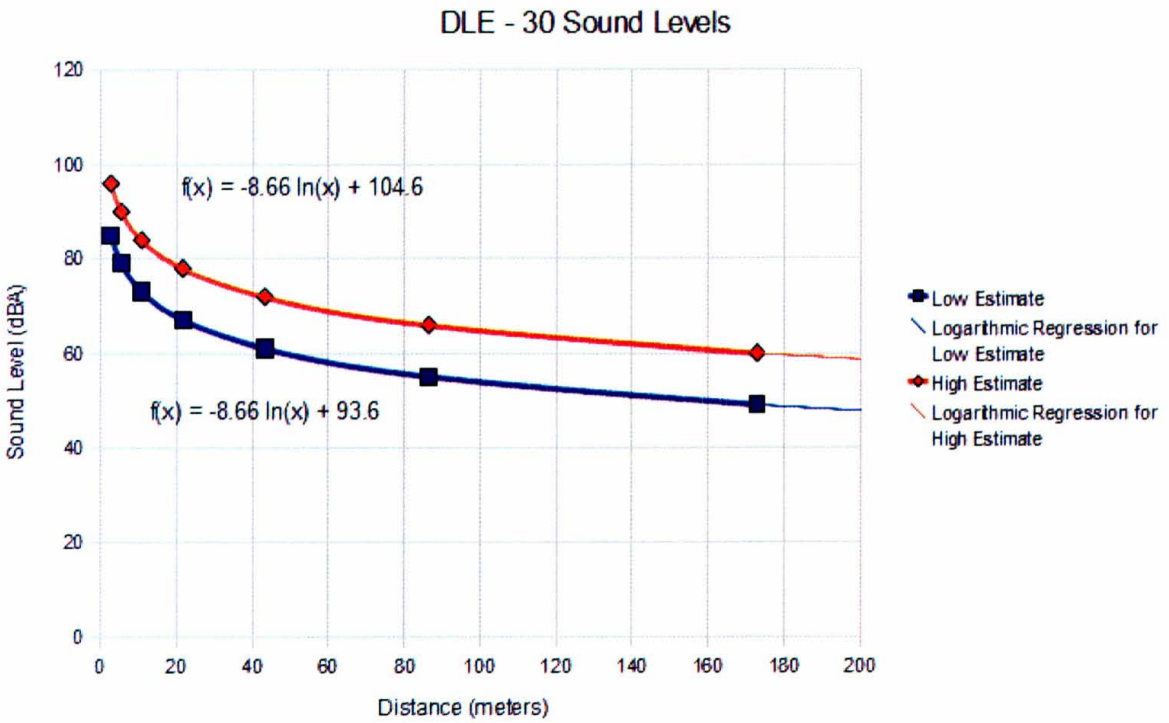

Figure 4-21: Car Horn Sound Levels: Graph shows the decrease in sound level observed as the distance from the sound source increases.

Chapter 5

Results

5.1 Tetrahedron Results

The result obtained from the phase correlation produced a series of 3D direction vectors; each vector corresponding to the location of the aircraft for each segment of audio used. This 3D direction is shown in Figure 5-4. Since the 3D direction is a product of the delays calculated for each of the microphone pairs, the direction is sensitive to the output of the phase correlation. As can be seen in Figures 5-1, 5-2 and 5-3, a trend is visible in each of the figures, however noise frequencies are also present. This noise interferes with the 3D direction vector calculation. In the case of the X-axis microphones and the Z-axis microphones, there appears to be a pattern to the noise. This pattern could be due to a second sound source in the vicinity of the microphone array, likely a gas powered generator that was in use at the time of the recording.

5.2 Ground and Air Tests

To reduce the noise present during the ground and air experiment, a microphone capsule was designed and built along with a mounting system. In order to test the

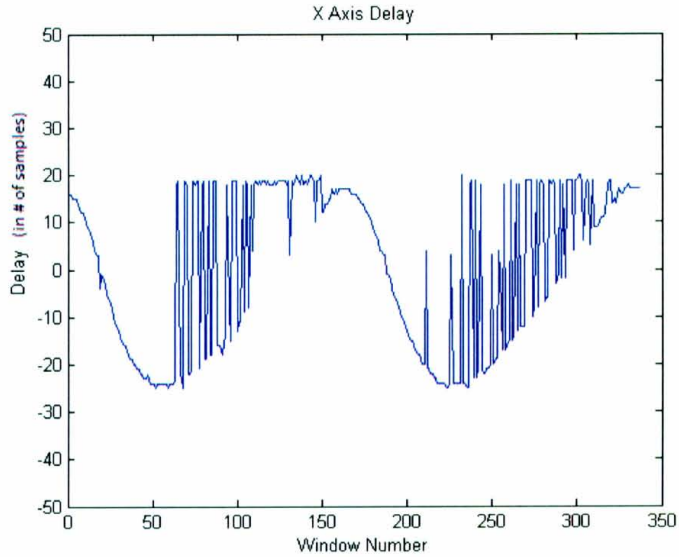

Figure 5-1: Delay found by phase correlation from X Axis Microphone

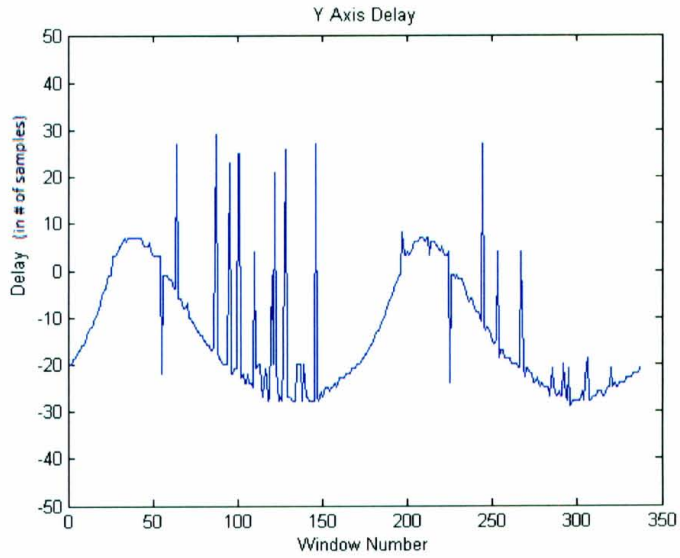

Figure 5-2: Delay found by phase correlation from Y Axis Microphone

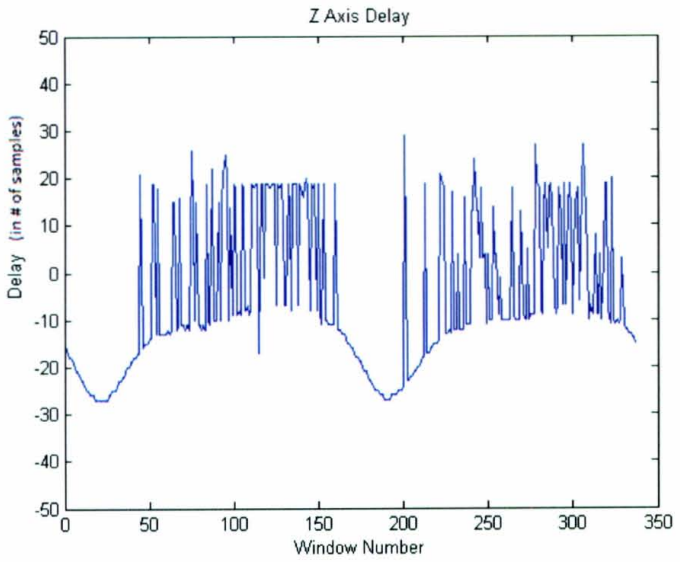

Figure 5-3: Delay found by phase correlation from Z Axis Microphone

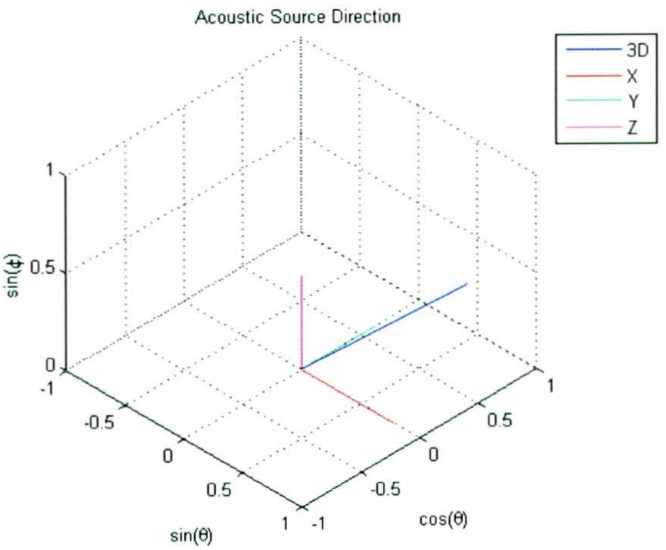

Figure 5-4: 3D sound source direction vector calculated, pointing in the direction of the aircraft as it travels.

Table 5.1: Microphone Capsule Ground Results

Speed (kmph)	Detection Distance (meters)	Sound Level (dBA)	Cessna Equivalent Distance (meters)
50	37.86 to 50.72	74.53 to 72	3834.05 to 5136.38
40	43.53 to 81.44	73.32 to 67.9	4408.25 to 8247.37
20	61.57 to 86.53	70.32 to 67.37	6235.15 to 8762.83

Table 5.2: Microphone Capsule Airborne Results

Speed (km/h)	Detection Distance (m)	Sound Level (dBA)	Cessna Equivalent Distance (m)
32	42	73	4761
			Shadow Equivalent Distance (m)
			500

effect of the microphone capsule. a ground test was designed to verify if the effect on the detection distance was significant. Following an airborne test was conducted to confirm that the microphone capsule could be used on board an aircraft.

During the ground experiment three variables were altered, the speed of the vehicle, the distance from the sound source as well as the microphone being used. All three of the variables were found to have a significant effect on the detection distance. The most significant effect was of course the speed of the vehicle. However the type of microphone used and separation also had a significant effect.

Further analysis was conducted on the detection distances. The values corresponding to the sound levels and the respective detection distances were extrapolated and compared to the sound levels produced by a manned aircraft. The aircraft chosen for comparison was a Cessna 182 as it is one of the most commonplace aircraft, and likely to be encountered during a UAS mission. Table 5.1 summarizes the expected distances that the Cessna would be detected at the different speeds for its recorded sound level. However, it must be emphasized the significant amounts of wind noise still present in the recordings. A significant step forward was made toward noise reduction pickup through design and manufacture of the aerodynamic microphone capsules.

Following, an airborne test was conducted to confirm the results of the ground test. For this experiment a DLE 30, 2 stroke engine was run at full throttle while a

small electrically powered aircraft, mounted with two microphone capsules, flew by. The detection distance was approximately 42 meters. The sound level for the DLE 30 at 40 meters is approximately 73 dBA; at this sound level the Cessna is approximated to be at a distance of 4761 meters, whereas a Shadow UAV would be approximately 500 meters away. These results are summarized in Table 5.2. For both the ground and airborne tests, the Cessna sound levels used for comparison were those reported by the U.S. Department of Transportation [8] during takeoff. As such, these results must be scaled down to reflect the sound levels produced while cruising, normally 75% thrust. As was mentioned for the ground test results, there are significant amounts of wind noise still present in the recordings. The aerodynamic microphone capsules improved the results, however the wind noise recorded was still strong and drowns out the sound source significantly.

Chapter 6

Conclusions and Future Work

The fundamental question is: is it possible to develop an acoustics based UAS detection system able to operate in adverse climatic/environmental conditions such as fog/smoke, to detect oncoming aircraft and provide the ability for successful avoidance?

6.1 Conclusions

This question was addressed. The three main experiments conducted were able to show that a sound source could be localized using an arrangement of 4 microphones. Furthermore, a ground test followed by an airborne test was conducted which showed a moving craft could detect the sound source. The detection distance was approximately 42 meters. Using the detection distances from the ground and airborne experiments, and the sound levels for manned aircraft, an estimate was made for the detection distance of a manned aircraft: a Cessna is approximated to be at a distance of 4761 meters, a Shadow UAV would be approximately 500 meters away.

Many challenges arose throughout this thesis. The most significant of which was wind noise. Wind socks are commercially available, however they are not aerodynamic and still result in high wind noise at high speeds. This challenge was tackled

by designing an aerodynamic capsule which would surround and contain a microphone, and hence decrease the buffeting of wind noise. Another challenge was the significant self noise produced by the engine/motor of the "sensing" craft, and vibrations from the aircraft. This was overcome by using an electric motor and shutting it off momentarily, and by dampening the vehicle's vibrations by using foam as an insulator. Smaller challenges encountered were that the smaller aircraft could not carry large computers, thus a smaller 4 channel recorder was used requiring offline processing to be conducted. As well, since not able to record manned aircraft and reliably determine the sound levels and distances, substitute sound sources were used such as a car horn and DLE - 30 engine. These alternative sound sources produced high enough sound levels to be able to conduct the experiments. One last challenge was the number of sensors able to be mounted on board the aircraft. Four microphones are required to localize a sound accurately. However, four microphones spaced approximately 1 foot apart requires a larger aircraft, and one of the microphones would inevitably be placed in the prop-wash of the aircraft. To overcome this, in this case only two microphones were used, placed on each side of the wing.

6.2 Future work

The next experiment that should be attempted is an autonomous flight with 2 airborne aircraft, one being an aircraft mounted with the DLE-30 engine and the other having 2 microphones mounted on either wing. The purpose of the experiment would be to confirm the results of the ground test as well as to collect airborne acoustic data from two completely autonomous aircraft.

A company mentioned in the introduction to this thesis, Microflown, is also conducting research into acoustic "sense and avoid" systems. A worthwhile comparison would be to test the performance of the microphone capsules designed in this thesis and the particle velocity sensor created by Microflown.

To further improve the performance of the microphone capsules, further optimization could be conducted on the profile of the aerofoil. A test could be made to maximize the angle of attack that will still produce laminar flow as well as the thickness and length of the boundary layer. Furthermore, different materials, such as carbon fiber, could be used to manufacture the capsules and tests conducted to compare their performance against the fiberglass capsules used in these experiments.

Ph.D. level extension of my research plan could be the integration into a real-time system for trajectory reconstruction of the intruding aircraft and danger level analysis. Collision detection can also be extended beyond UAVs to manned aircraft. As well, co-operative systems such as ADSB could be used in conjunction with the microphones to conduct tests with manned aircraft to obtain distance information on the crafts being recorded.

Bibliography

[1] K. Ellis, "Investigation of emerging technologies and regulations for uav sense and avoid capability," *National Research Council, Institute for Aerospace Research*, vol. Report LTR-FR-258, October 2006.

[2] B. C. Karhoff, J. I. Limb, S. W. Oravsky, and A. D. Shephard, "Eyes in the Domestic Sky: An Assessment of Sense and Avoid Technology for the Army's Warrior Unmanned Aerial Vehicle," *Systems and Information Engineering Design Symposium, 2006 IEEE*, pp. 36–42, Apr. 2006.

[3] C. Le Tallec, "VFR general aviation aircraft and UAV flights deconfliction," *Aerospace Science and Technology*, vol. 9, pp. 495–503, Sept. 2005.

[4] R. J. Fontana, "Recent system applications of short-pulse ultra-wideband (UWB) technology," *IEEE Transactions on Microwave Theory and Techniques*, vol. 52, pp. 2087–2104, Sept. 2004.

[5] U. Ingard, "A review of the influence of meteorological conditions on sound propagation," *The Journal of The Acoustical Society of America*, vol. 25, no. 3, p. 405, 1953.

[6] C. M. Harris, "Absorption of sound in air versus humidity and temperature," *The Journal of The Acoustical Society of America*, vol. 40, p. 148, 1966.

[7] Stryker Brigade Combat Team, "Aircraft noise emission estimates," *Draft EIS, Hawaii*, 2003.

[8] U.S. Department of Transportation, "Estimated airplane noise levels in a-weighted decibels," Tech. Rep. 36-3H, Federal Aviation Administration, 2002.

[9] L. Zhou, "A precise underwater acoustic positioning method based on phase measurement," Master's thesis, University of Victoria, 2010.

[10] B. C. Kirkwood, "Acoustic source localization using time-delay estimation," Master's thesis, Technical University of Denmark, 2003.

[11] J. S. Bendat and A. G. Piersol, *Engineering Applications of Correlation and Spectral Analysis*. New York: Wiley, second ed., 1993. First edition: 1980.

[12] A. Akbari, N. Yousefian, and M. Rahmani, "Sound source localization in 3-d space by a triple-microphone algorithm," in *14th Asia-Pacific Conference on Communications*, 2008.

[13] A. Quach and K. Lo, "Automatic target detection using a ground-based passive acoustic sensor," *IEEE*, vol. 99, pp. 187 – 192, 1999.

[14] F. Dommermuth, "Estimation of fundamental frequencies," *Radar and Signal Processing, IEE Proceedings F*, vol. 140, no. 3, pp. 162–170, 1993.

[15] Rycote.com, "Miniscreen windjammer." http://www.rycote.com/products/miniscreen/, 2012.

[16] H.-E. de Bree and G. de Croon, "Acoustic vector sensors on small unmanned air vehicles," *Micro Air Vehicle Laboratory, Delft University of Technology, the Netherlands*, 2011.

[17] E. Tijs, G. de Croon, J. Wind, B. Remes, C. de Wagter, H.-E. de Bree, and R. Ruijsink, "Hear-and-avoid for micro air vehicles," *International Micro Air Vehicle Conference and Competitions (IMAV 2010)*, 2010.

[18] T. Milkie, "UAV Sense and Avoid Using the PANCAS System." SARA Inc., July 2008.

[19] Scientific Applications & Research Associates, Inc, "Acoustic sensors for unmanned air vehicles." `http://www.sara.com/ISR/acoustic_sensing/LOSAS.html`, 03 2012.

[20] C. Pozrikidis, *Fluid Dynamics: Theory, Computation, and Numerical Simulation.* Springer Science, 2009.

[21] P. Marzocca, "The NACA Airfoil Series." `http://people.clarkson.edu/~pmarzocc/AE429/The%20NACA%20airfoil%20series.pdf`, 2003.

[22] L. Charles L., J. Cuyler W. Brooks, H. Acquilla S., and S. Darrell W., "Computer Program to Obtain Ordinates for NACA Airfoils," tech. rep., National Aeronautics and Space Administration, Langley Research Center, 1996.

[23] D. C. Montgomery, *Design and Analysis of Experiments.* John Wiley & Sons, 2006.

[24] M. Hepperle, *Java Foil.* http://www.mh-aerotools.de/airfoils/javafoil.htm, 2006.

[25] K. Steemers and S. Yannas, *Architecture, city, environment: proceedings of PLEA 2000 : July 2000, Cambridge, United Kingdom.* James & James, 2000.

[26] E. Berger, *The Noise Manual.* American Industrial Hygiene Association, 2003.

Appendix A

Diagrams

A.1 Microphone Capsule Design and Manufacture

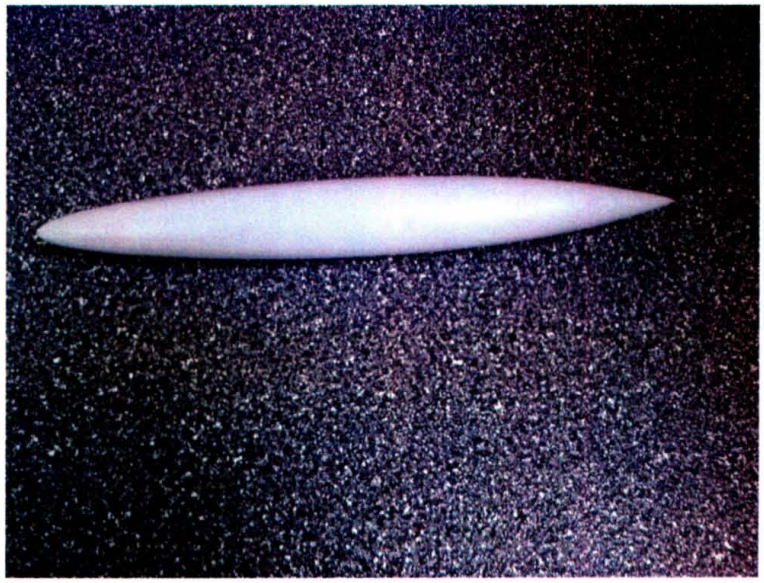

Figure A.1: 3D Printed NACA Airfoil: Printed using a rapid prototype machine, sprayed with a filler and sanded.

Figure A.2: Completed Mold (Top and Bottom)

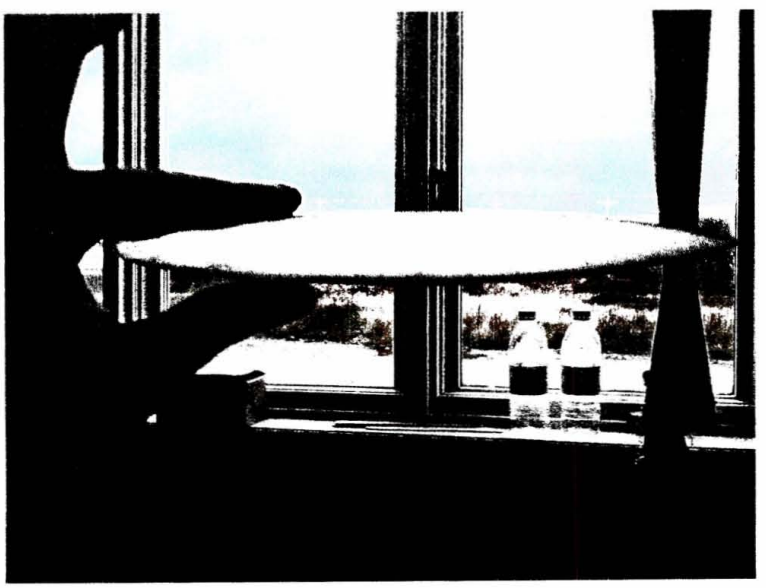

Figure A.3: Microphone Capsule

A.2 Spectrograms of GoPro and Capsule audio recordings

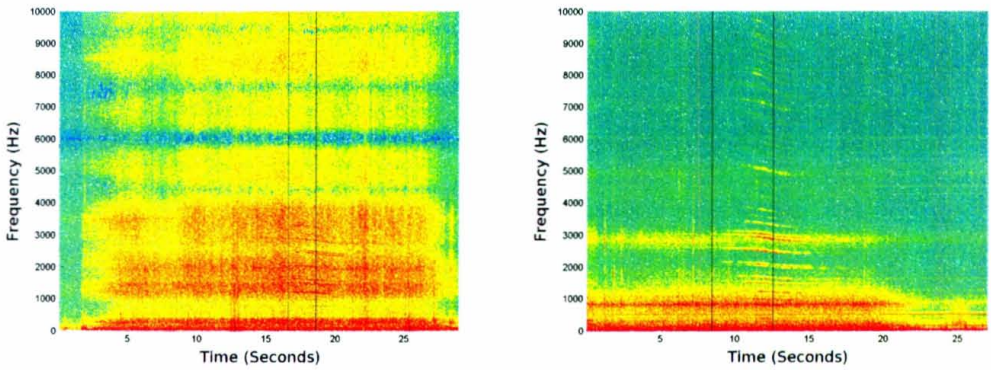

(a) goPro (b) Microphone Capsule

Figure A.4: Spectrogram comparison of goPro and capsule at 40 kilometres per hour and 10 meter separation. First line is point of detection, second line is point of closest approach.

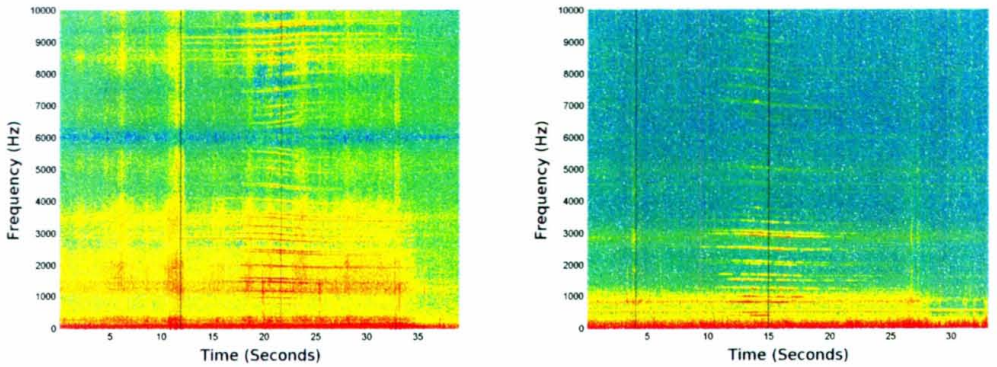

(a) goPro (b) Microphone Capsule

Figure A.5: Spectrogram comparison of goPro and capsule at 20 kilometres per hour and 10 meter separation

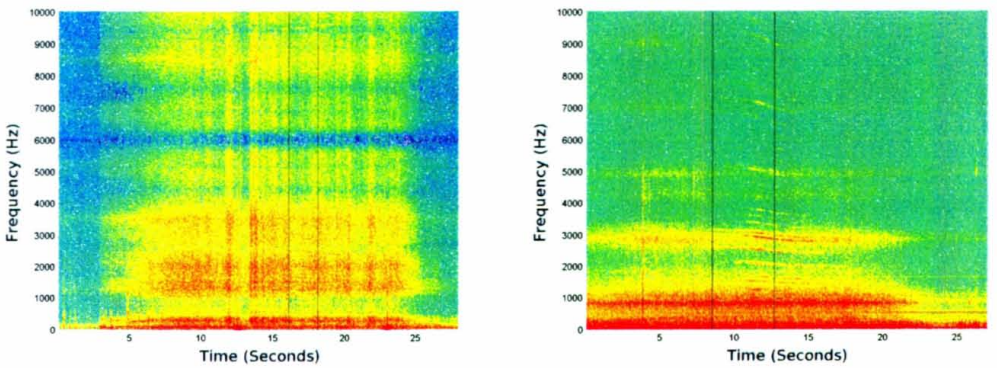

(a) goPro (b) Microphone Capsule

Figure A.6: Spectrogram comparison of goPro and capsule at 50 kilometres per hour and 20 meter separation

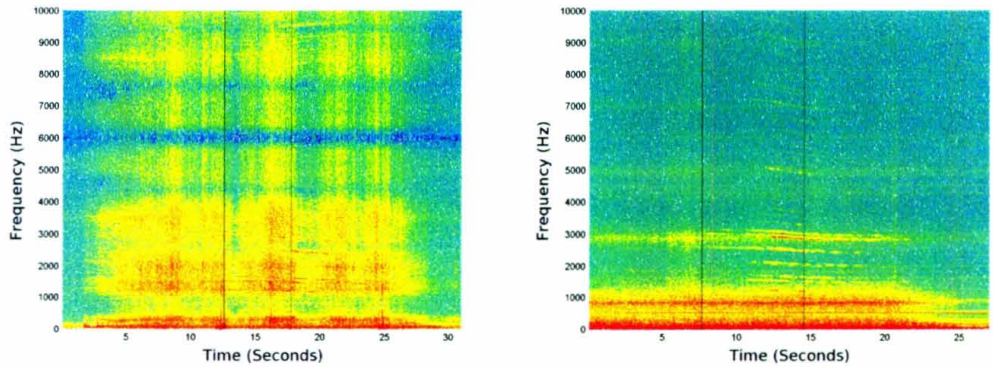

(a) goPro (b) Microphone Capsule

Figure A.7: Spectrogram comparison of goPro and capsule at 40 kilometres per hour and 20 meter separation

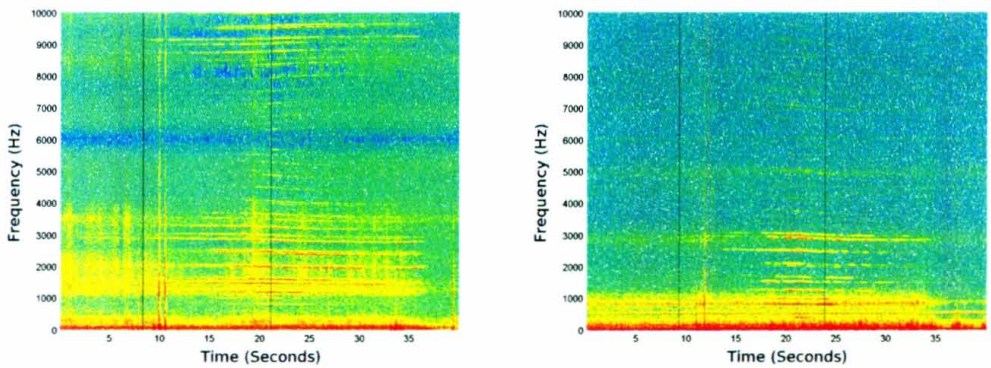

(a) goPro (b) Microphone Capsule

Figure A.8: Spectrogram comparison of goPro and capsule at 20 kilometres per hour and 20 meter separation

A.3 Design Expert Diagrams

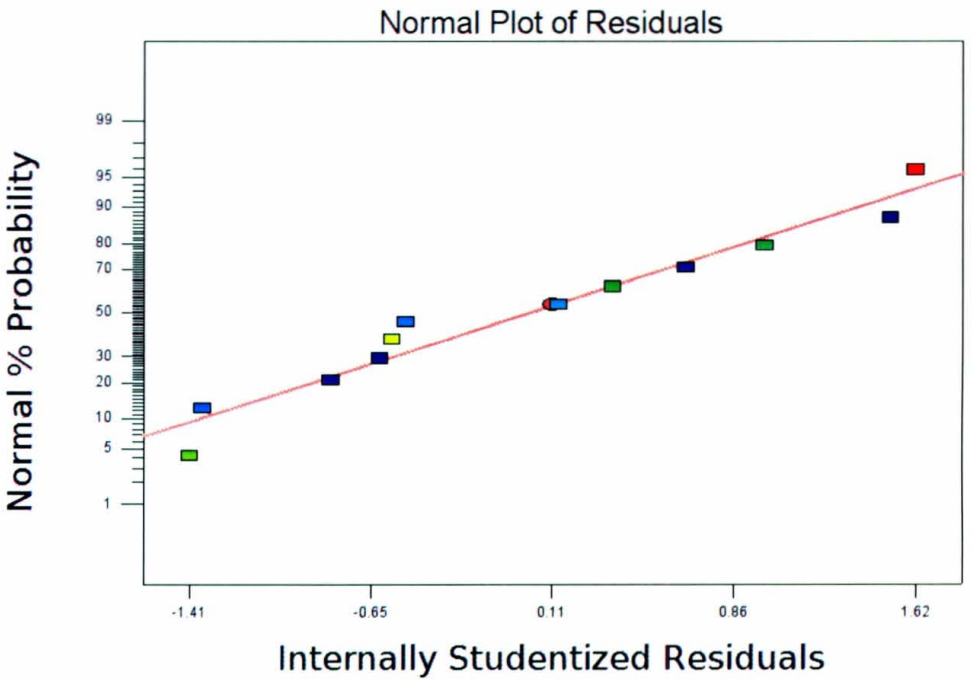

Figure A.9: Normal Plot of Residuals

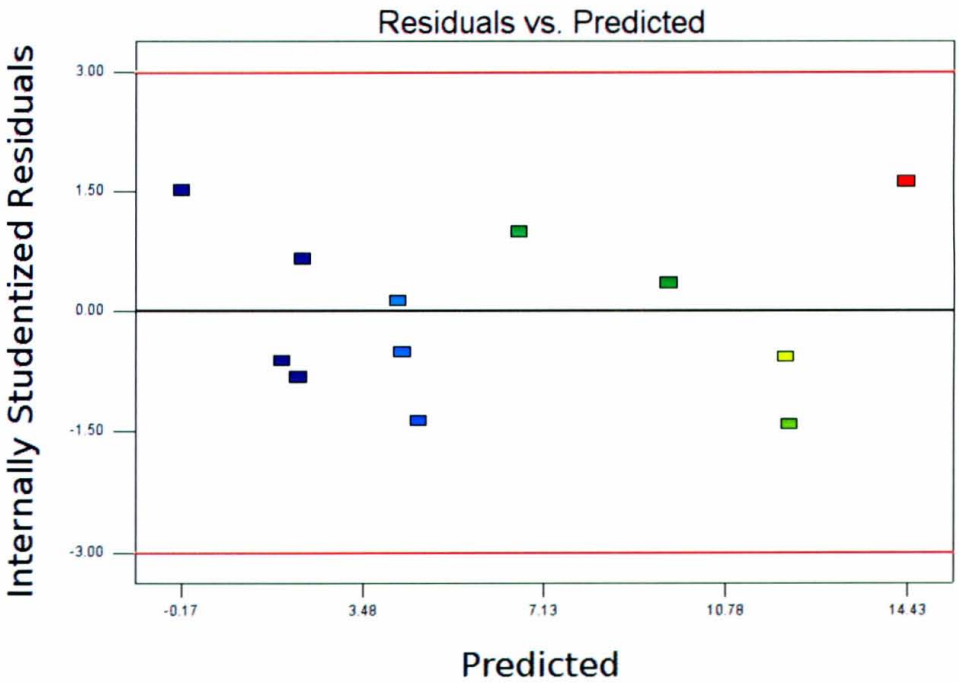

Figure A.10: Residuals vs Predicted

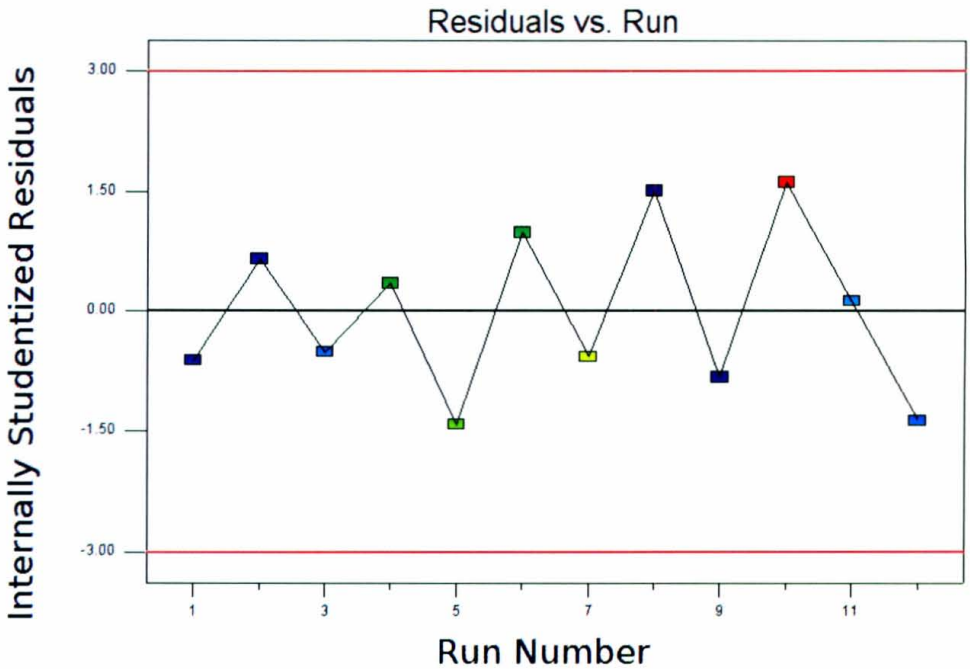

Figure A.11: Residuals vs Run

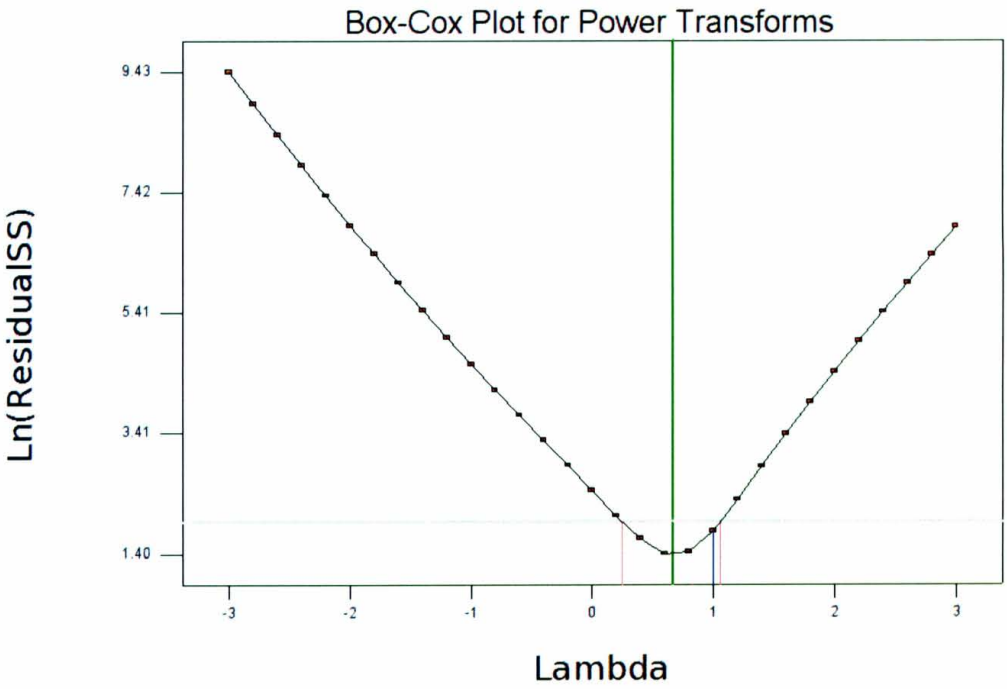

Figure A.12: Box Cox Plot

Appendix B

Equipment Used

B.1 Tetrahedron Experiment

- H2 Zoom Handy Recorder
- Giant Big Stick with Gasoline Engine
- Barometer
- Anemometer
- H2 Zoom Handy Recorder

B.2 Ground Experiment

- H2 Zoom Handy Recorder
- Barometer
- Anemometer
- Signal Generator
- Speakers

- GPS Recorder
- Car Horn
- 2 GoPro Cameras

B.3 Airborne Experiment

- H2 Zoom Handy Recorder
- Giant Big Stick with DLE 30 Gasoline Engine
- Ultra Stick with mounted microphones
- Barometer
- Anemometer
- GPS Recorder